GEOLOGICA CARPATHICA, AUGUST 2019, 70, 4, 325–354 doi: 10.2478/geoca-2019-0019

Integrated bio- and cyclostratigraphy of Middle Triassic (Anisian) ramp deposits, NW Bulgaria

GEORGE AJDANLIJSKY[1], ANDRÉ STRASSER[2] and ANNETTE E. GÖTZ[3,✉]

[1]University of Mining and Geology "St. Ivan Rilski", Department of Geology and Geoinformatics, Sofia 1700, Bulgaria; g.ajdanlijsky@mgu.bg
[2]University of Fribourg, Department of Geosciences, Geology–Paleontology, 1700 Fribourg, Switzerland; andreas.strasser@unifr.ch
[3]University of Portsmouth, School of Earth and Environmental Sciences, Portsmouth PO1 3QL, United Kingdom;
✉annette.goetz@port.ac.uk

(Manuscript received March 18, 2019; accepted in revised form June 27, 2019)

Abstract: A cyclostratigraphic interpretation of peritidal to shallow-marine ramp deposits of the early Middle Triassic (Anisian) Opletnya Member exposed in outcrops along the Iskar River gorge, NW Bulgaria, is presented. Based on facies trends and bounding surfaces, depositional sequences of several orders can be identified. New biostratigraphic data provide a time frame of the studied succession with placement of the boundaries of the Anisian substages and show that the Aegean (early Anisian) substage lasted about 1.6 Myr. In the corresponding interval in the two studied sections, 80 elementary sequences are counted. Five elementary sequences compose a small-scale sequence. The prominent cyclic pattern of the Opletnya Member can thus be interpreted in terms of Milankovitch cyclicity: elementary sequences represent the precession (20-kyr) cycle and small-scale sequences the short eccentricity (100-kyr) cycle in the Milankovitch frequency band. Medium-scale sequences are defined based on lithology but only in two cases can be attributed to the long eccentricity cycle of 405 kyr. The transgressive-regressive facies trends within the sequences of all scales imply that they were controlled by sea-level changes, and that these were in tune with the climate changes induced by the orbital cycles. However, the complexity of facies and sedimentary structures seen in the Opletnya Member also implies that additional factors such as lateral migration of sediment bodies across the ramp were active. In addition, three major sequence boundaries have been identified in the studied sections, which can be correlated with the boundaries Ol4, An1, and An2 of the Tethyan realm.

Keywords: Sedimentary cycles, palynology, conodonts, Triassic, Western Balkanides, NW Bulgaria.

Introduction

The Anisian is a crucial time interval in Earth's history to understand carbonate platform reorganization in the aftermath of the most severe extinction event at the end of the Permian (e.g., Benton 2015) and the incipient break-up of the supercontinent Pangaea (Stampfli et al. 2013), the northwestern Tethyan realm being best suited to study the comeback of shallow-marine environments at the beginning of the Mesozoic (e.g., Feist-Burkhardt et al. 2008; Stefani et al. 2010; Haas et al. 2012; Escudero-Mozo et al. 2015; Matysik 2016; Chatalov 2018).

Since the first detailed descriptions in the late 19th century by Toula (1878), Middle Triassic carbonate successions of the Western Balkanides have been studied to define lithostratigraphic units and detect facies types (Tronkov 1960, 1968, 1973, 1976, 1981, 1992; Tronkov et al. 1965; Chemberski et al. 1974; Assereto & Čatalov 1983; Assereto et al. 1983; Chatalov 1997; Benatov & Chatalov 2000; Chatalov et al. 2001). Microfossils and invertebrate groups have been used (Tronkov 1968, 1976; 1983, 1995; Budurov & Stefanov 1972; Budurov 1980; Budurov & Trifonova 1995; Benatov 2000, 2001) to compare and correlate these deposits referred to as "Balkanide type" (Ganev 1974; Chatalov 1980, 1991; Zagorchev & Budurov 2009) lithologically and stratigraphically with the "Germano-type" Muschelkalk successions of the Germanic Basin, showing striking facies similarities (Chatalov 1991). However, up to date the lack of a robust biostratigraphic framework hampers a precise age control of these deposits and hence regional correlation with Middle Triassic ramp systems of the northwestern Tethyan (e.g., Michalík et al. 1992; Haas et al. 1995; Philip et al. 1996; Török 1998; Götz et al. 2003; Rychliński & Szulc 2005; Götz & Török 2008) and Peri-Tethyan, i.e. Germanic realms (e.g., Götz 1996; Szulc 2000; Pöppelreiter 2002; Borkhataria et al. 2006; Matysik 2016). The challenge of a high-resolution correlation of Anisian Muschelkalk ramp cycles across the Tethyan shelf and the Peri-Tethyan basin was outlined by Götz & Török (2018).

Recent studies revisited the excellent outcrops along the Iskar River gorge (Fig. 1), focusing on the continental–marine transition and ramp initialization (Ajdanlijsky et al. 2018), and on the overall facies development of the ramp system (Chatalov 2013, 2018). The onset of the Anisian ramp system, after continental sedimentation in the Early Triassic, features a pronounced cyclic character of peritidal and shallow-marine carbonates (Chatalov 2000), and different hierarchical scales can be defined for the Early to early Middle Triassic interval. A major sequence boundary occurs at the base of the Middle Triassic Iskar Carbonate Group (Ajdanlijsky et al. 2018). A mid-Anisian maximum-flooding zone is inferred from

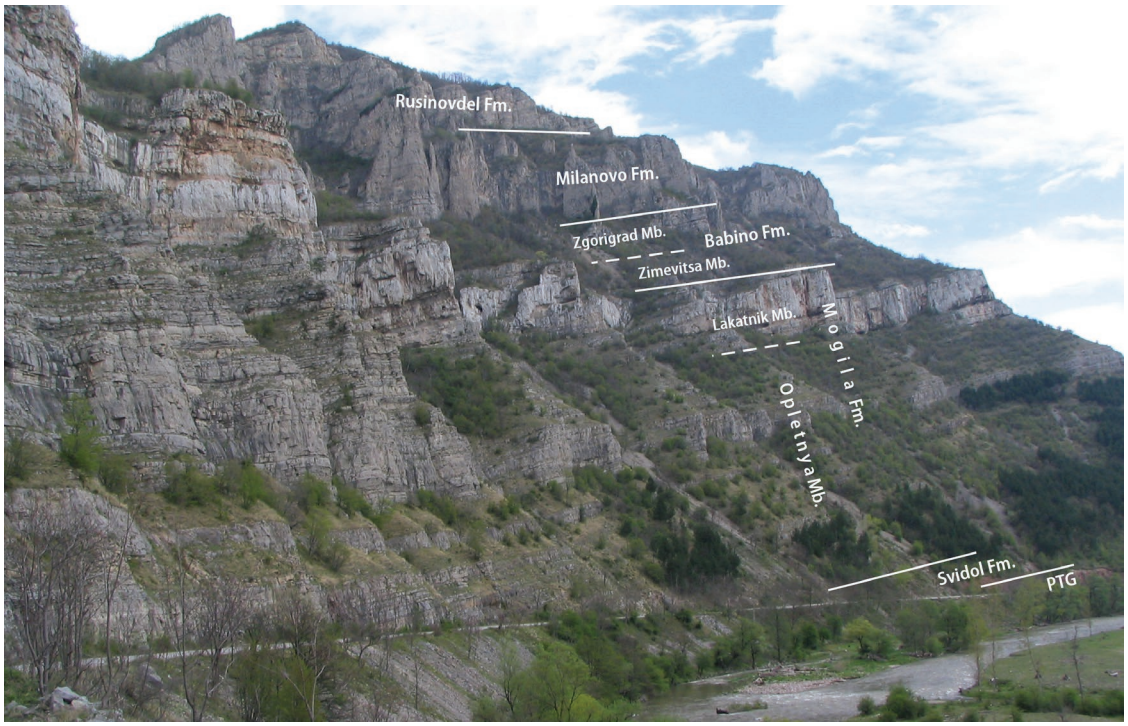

Fig. 1. Excellent outcrops along the Iskar River gorge expose the Iskar Carbonate Group overlying the Petrohan Terrigenous Group (PTG). The Opletnya Member is ca. 135 m thick.

the litho- and biofacies of the so-called "Terebratula Beds" (Chatalov 2013), and a long-term, second-order sea-level rise is interpreted from the Olenekian onwards, followed by a mid-Anisian to early Carnian sea-level fall again creating a major sequence boundary (Chatalov 2018).

The present study yields new biostratigraphic data providing a refined age control. Palynofacies analysis is used to decipher short- and long-term sea-level fluctuations by changes of terrigenous input, preservation and sorting of phytoclasts, and prominent phytoplankton (acritarch) peaks indicating major flooding phases. Combined with the detailed analysis of lithology and sedimentary structures, this allows a robust sequence- and cyclostratigraphic interpretation to be proposed.

Geological setting

The study area, located approximately 35 km north of Sofia, is part of the Western Balkanides, i.e. the Western Balkan Tectonic Zone (Ivanov 1998) of the Alpine orogenic belt. Its pre-Mesozoic basement includes high-grade metamorphosed lower Paleozoic sedimentary and igneous rocks and upper Paleozoic sedimentary, igneous and volcanic rocks (Yanev 2000). The overlying Triassic succession forms the base of the Mesozoic cover and is subdivided into three units: the Petrohan Terrigenous Group (Tronkov 1981) consisting predominantly of fluvial deposits; the Iskar Carbonate Group (Tronkov 1981) composed of shallow-marine carbonates and mixed siliciclastic–carbonate rocks; and the Moesian Group (Chemberski et al. 1974) represented by siliciclastic–carbonate and carbonate rocks (Fig. 2). The Iskar River gorge exposes an excellent continuous succession of the marine Iskar Carbonate Group with a maximum thickness of about 480 m (Chatalov 2013). The lower part of the group is assigned to the Anisian stage (Fig. 3).

Materials and methods

Two key sections (Lakatnik and Sfrazen) of the Mogila Formation as part of the Iskar Carbonate Group (Figs. 2, 3) were logged in great detail. The Sfrazen section, representing the formation's type section, is situated north of Sfrazen hamlet, 1.5 km west of the village of Opletnya. The Lakatnik section is located directly north of the Lakatnik railway station, about 3 km west of the Sfrazen hamlet. Both sections offer excellent lateral and almost continuous vertical exposures of the Mogila Formation. The detailed bed-by-bed documentation includes lithology, fossil content, and sedimentary structures. The microfacies and the textures (Dunham classification) were determined on the outcrop with a hand lens and in 52 thin-sections. In the Sfrazen section, the overlying Babino Formation and lowermost Milanovo Formation were logged in order to obtain additional biostratigraphic tie points. Samples for biostratigraphic analysis of palynomorphs and conodonts, and for palynofacies analysis were taken from all three formations and different lithologies. In both sections, a small-scale cycle within the lower Mogila Formation (Opletnya Member) was sampled for high-resolution palynofacies analysis.

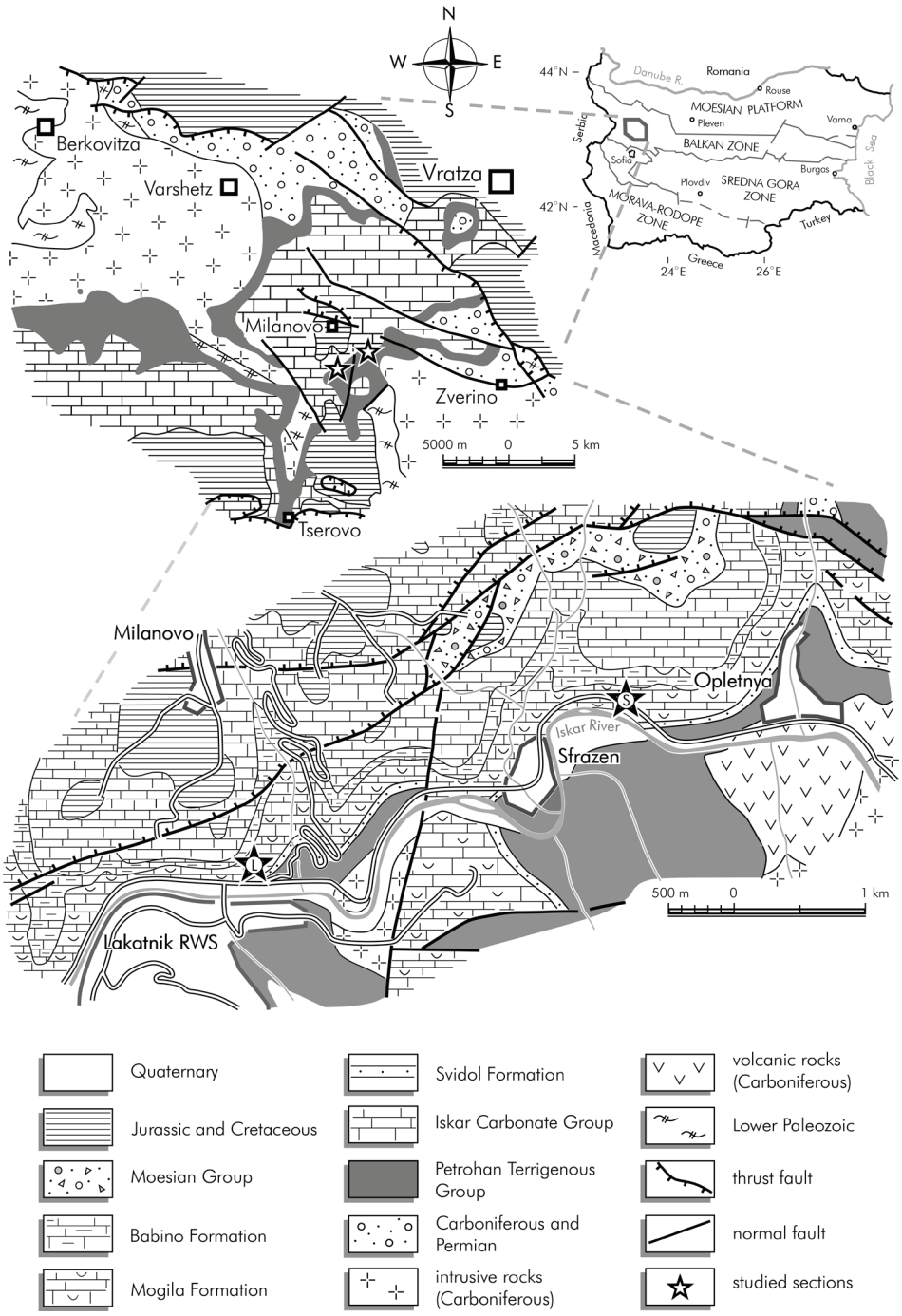

Fig. 2. Study area and location of studied sections north of Sofia in the Balkan Zone, NW Bulgaria (modified from Ajdanlijsky et al. 2018). L: Lakatnik section (43°05'22" N, 23°23'34" E); S: Sfrazen section (43°06'04" N, 23°25'27" E).

Palynological samples were prepared using standard processing techniques (Wood et al. 1996), including HCl (33 %) and HF (73 %) treatment for dissolution of carbonates and silicates, and saturated $ZnCl_2$ solution (D≈2.2 g/ml) for density separation. Residues were sieved at 15 μm mesh size and mounted in Eukitt, a commercial, resin-based mounting medium. Palynological slides were analyzed on a Leica DM2000 microscope. Formic acid (10 %) was used for extraction of conodont elements from bioclastic grainstones. After sieving the residue, conodont elements were picked and transferred to microcells for identification using a Leica M80 stereomicroscope.

Biostratigraphy

Early biostratigraphic studies on the Bulgarian Triassic used conodonts to establish a zonation scheme applicable for

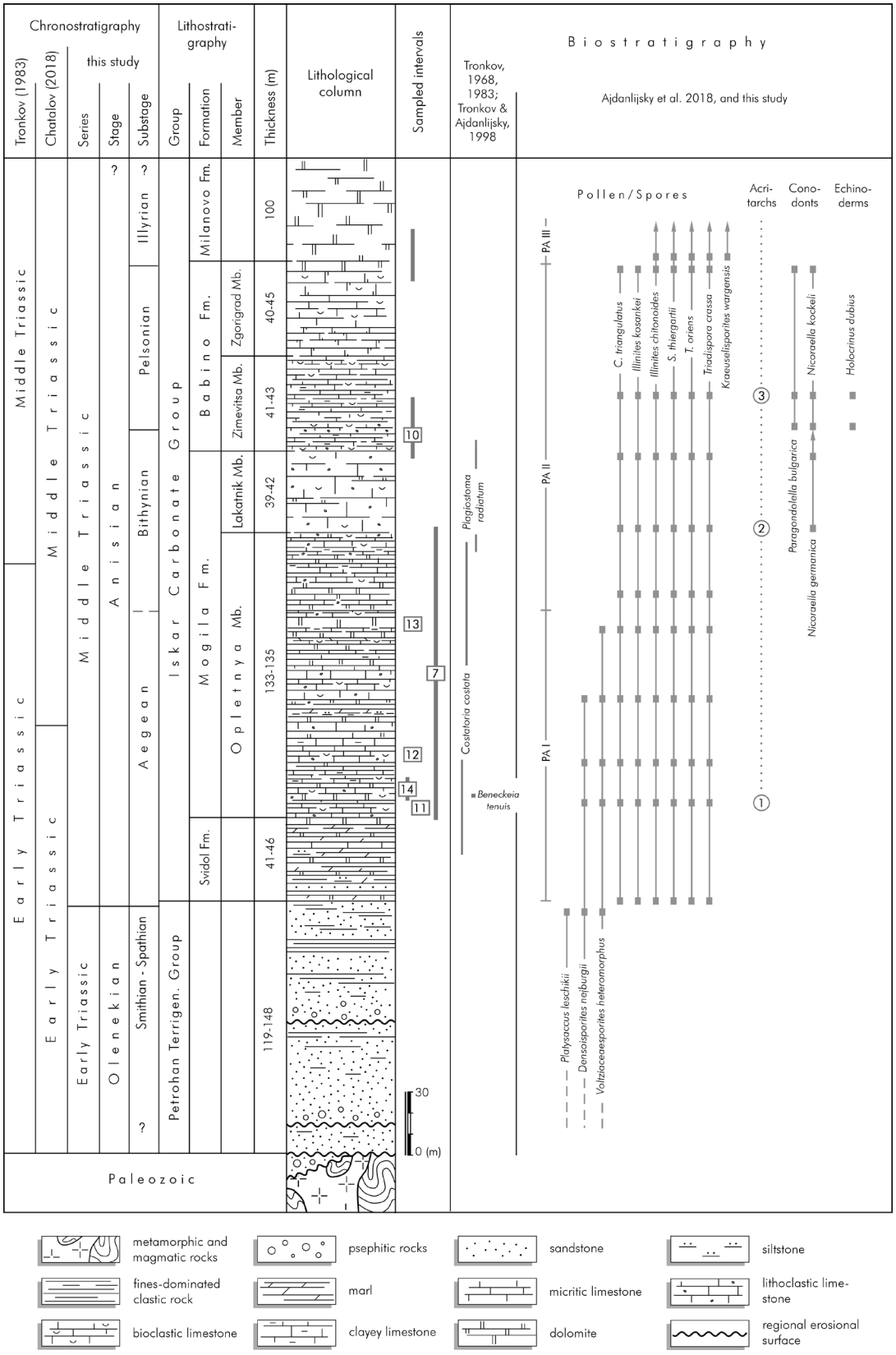

Fig. 3. Stratigraphy of the Triassic sequence exposed in outcrops of the Iskar River gorge, NW Bulgaria, with range of the studied sections shown in Figures 7, 10, 11, 12, 13, and 14. The placement of the Olenekian–Anisian boundary and the Anisian substage boundaries is based on new biostratigraphic data (Ajdanlijsky et al. 2018; this study). Acritarch peaks occur in the lower Opletnya Member (1), lower Lakatnik Member (2), and Zimevitsa Member (3), indicating major flooding events. Abbreviations: Fm.=Formation, Mb.=Member; PA I=palynoassemblage I (Aegean), PA II=palynoassemblage II (Bithynian–Pelsonian), PA III=palynoassemblage III (Illyrian).

the marine parts of the succession (Budurov & Stefanov 1972, 1973, 1975; Budurov 1976, 1980). They were later accompanied by analyses of benthic foraminiferal assemblages, firstly to erect a refined zonation scheme including standard conodont and foraminifera zones (Budurov & Trifonova 1984, 1995; Budurov et al. 1995), and secondly to provide a tentative correlation with the Tethyan ammonite zones. Studies by Tronkov (1960, 1968, 1981, 1983) focused on invertebrate groups, mainly bivalves and brachiopods, and also used rare ammonoid findings (Tronkov 1976) to overcome the limited correlation of the Bulgarian Triassic with the Triassic of the Tethyan and Peri-Tethyan realms. Later, Benatov (1998) established regional bivalve and brachiopod zones for the Middle Triassic in order to correlate them with the existing zonation schemes. Consequently, these zones were used for dating and regional correlation (Benatov et al. 1999; Benatov 2000, 2001). However, the facies-dependent occurrence of bivalves and brachiopods and their generally low time resolution hampers precise dating and correlation at regional and over-regional scales. Furthermore, conodont assemblages obtained from olistoliths (Budurov 1976) without reference sections, the noticeable conodont provincialism (Budurov & Petrunova 2000) and Peri-Tethyan endemism (Chen et al. 2019), and ultimately the huge recent progress in Triassic conodont research applying multi-element taxonomy and revised, lineage-based zonation schemes (e.g., Chen et al. 2015, 2019), demonstrate the urgent need of a revision of the existing conodont stratigraphy of Bulgaria.

Previous palynological investigations in the Triassic of Bulgaria have been limited to a few attempts to date formations (Kalvacheva & Čatalov 1974; Čatalov & Visscher 1990; Petrunova 1992a,b, 1999, 2000; Budurov et al. 1997). However, recent palynological studies on continental and marine deposits of the Early–Middle Triassic transition interval exposed in outcrops along the Iskar River gorge (Ajdanlijsky et al. 2018) show the huge potential to establish a high-resolution palynostratigraphy. So far, the Olenekian–Anisian boundary was palynologically identified in the uppermost fluvial Petrohan Terrigenous Group, differing from previous interpretations, which placed this boundary at different positions in the Mogila Formation of the overlying Iskar Carbonate Group (Tronkov 1983; Chatalov 2018). In the present study, the focus is on palynomorphs to further develop Triassic palynostratigraphy. Additionally, conodonts are used to refine the existing Anisian stratigraphy of NW Bulgaria.

Palynological key taxa allow dividing the Anisian succession into three palynoassemblages (Fig. 3). Assemblage I identified in the lower Mogila Formation is characterized by Anisian index taxa including *Cristianisporites triangulatus*, *Illinites kosankei*, *Illinites chitonoides*, *Stellapollenites thiergartii*, *Tsugaepollenites oriens,* and *Triadispora crassa*. Early Triassic elements such as *Densoisporites nejburgii* and *Voltziaceaesporites heteromorphus* are still present, indicating an early Anisian (Aegean) age (Heunisch 1999, 2019). Assemblage II is composed of Anisian taxa as listed above, with the last appearance of *Cristianisporites triangulatus* and *Illinites kosankei* in the uppermost Babino Formation, indicating a Bithynian–Pelsonian age. Assemblage III of the basal Milanovo Formation is characterized by *Illinites chitonoides*, *Stellapollenites thiergartii*, *Tsugaepollenites oriens*, *Triadispora crassa,* and the first appearance of *Kraeuselisporites wargensis*, indicating a late Anisian (Illyrian) age (Kustatscher & Roghi 2006).

In the Sfrazen section, the occurrence of conodonts (*N. germanica*/*N. kockeli*) in the upper Mogila Formation and the Babino Formation enables the placement of the Bithynian/Pelsonian boundary (Götz et al. 2019) in the lowermost Zimevitsa Member of the Babino Formation. The identification of Pelsonian elements such as *Paragondolella bulgarica* (Chen et al. 2015), accompanied by findings of crinoid columnal segments of *Holocrinus dubius*, an index species of the Pelsonian (Hagdorn & Głuchowski 1993; Głuchowski & Salamon 2005; Niedźwiedzki & Salamon 2006), in bioclastic grainstones of the Zimevitsa Member, support this age assignment.

Sedimentology

In the studied area, the Anisian succession starts with the Svidol Formation that demonstrates a wide variety of siliciclastic–terrigenous, siliciclastic–carbonate, and carbonate rocks (Ajdanlijsky et al. 2018), followed upwards by the mainly carbonate successions of the Mogila, Babino and Milanovo formations.

Opletnya Member

In the Opletnya Member (lower part of the Mogila Formation), carbonates prevail while the mixed siliciclastic–terrigenous and siliciclastic–carbonate rocks, presented mainly by thin beds, form only an insignificant part of the succession. Among the carbonates, where limestones prevail over dolomitic limestones and dolomites, wacke- and packstones are more common than mud- and grainstones.

Wackestones and mudstones

Wacke- and mudstones are medium- to thick-bedded (15–80 cm), rarely thin-bedded (5–8 cm), massive, laminated or nodular (Fig. 4b), commonly bioturbated (Figs. 4a, 5a), and contain benthic foraminifera and ostracods. The laminations are more often thick (3–4 mm) than thin (1–1.5 mm). In some cases, scale and intensity of the bioturbation allows for lateral correlation between sections. Pebble-sized intraclasts, mainly with lithologies similar to those of the hosting bed, occur very rarely. Solitary small fragments of gagate (jet) are observed in several levels (Zdravkov et al. 2019). Birdseyes and different degrees of dolomitization occur occasionally both in wackestones and mudstones. These facies and sedimentary structures point to a peritidal to shallow-marine environment (e.g., Flügel 2004).

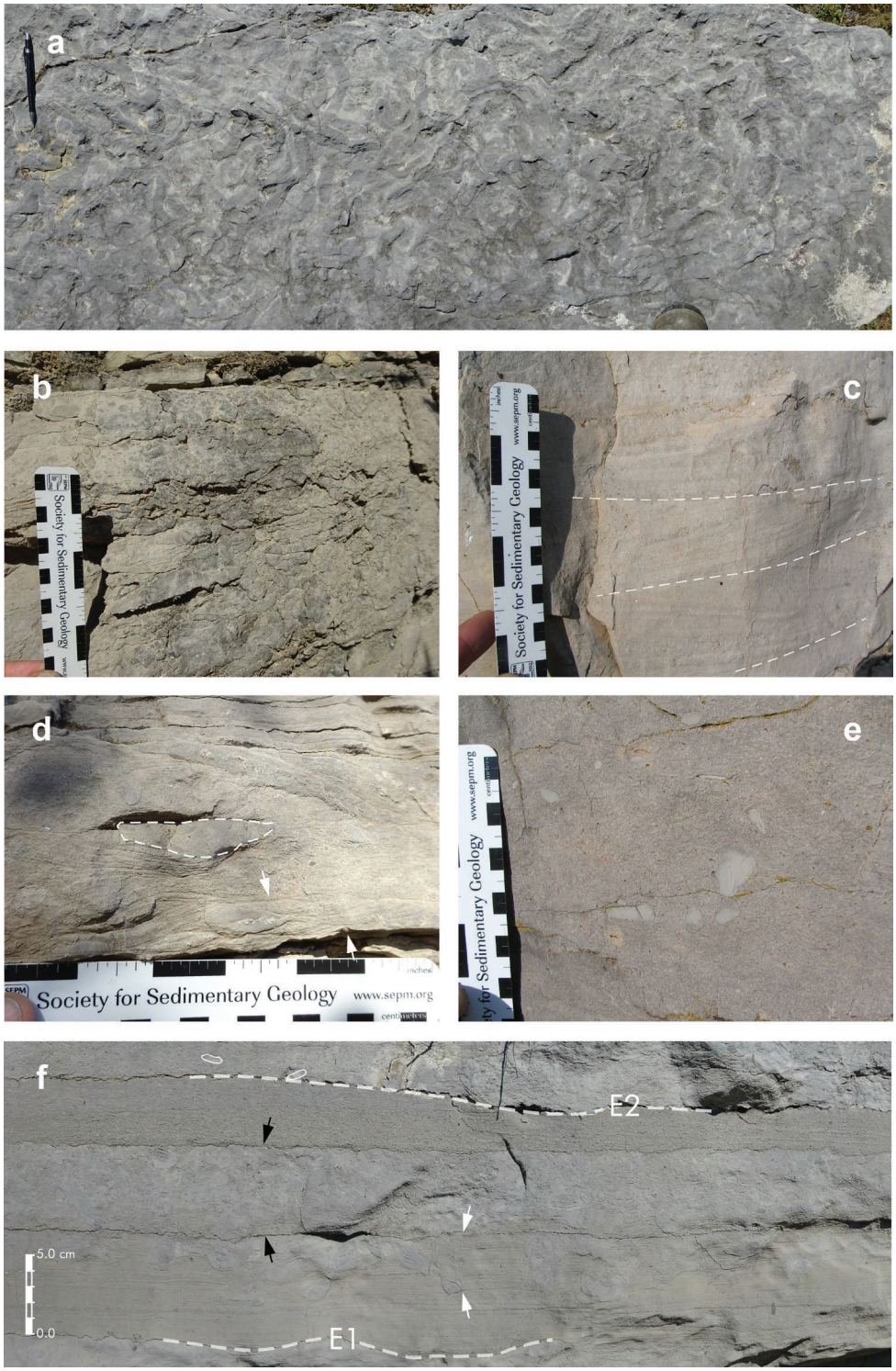

Fig. 4. Limestone lithologies in the Opletnya Member (Mogila Formation): **a** — plan view of intensively bioturbated wackestone (pen for scale), Sfrazen section, 86.6 m, elementary sequence 44; **b** — nodular wacke- to mudstone from the lower part of the Opletnya Member, Sfrazen section, 53.2 m, elementary sequence 25; **c** — trough cross-bedded grainstone, uppermost part of the Opletnya Member, Lakatnik section, 128.8 m, elementary sequence 67; **d** — cross-bedded packstone with prograding coset of small-scale planar cross-bedding (between arrows), angular and rounded intraclasts (surrounded) in lower part, and reactivation surface above. Lower part of highstand deposits, Sfrazen section, 51.5 m, elementary sequence 25; **e** — massive packstone with rounded, pebble-sized intraclasts from the lowermost part of the Opletnya Member, Sfrazen section, 2.8 m, elementary sequence 2; **f** — transgressive package of bioclastic, horizontally laminated packstone partially (between white arrows) to almost completely (between black arrows) bioturbated, with isolated pebble-sized intraclasts (outlined) along a small-scale erosional surface (E2, dashed line). A similar erosional surface (E1), cutting into slightly bioturbated and dolomitic limestone, marks the base of an elementary sequence. Sfrazen section, 81.6 m, elementary sequence 41. The position in meters is given starting from the base of the Opletnya Member, the numbering of the elementary sequences is according to Fig. 7.

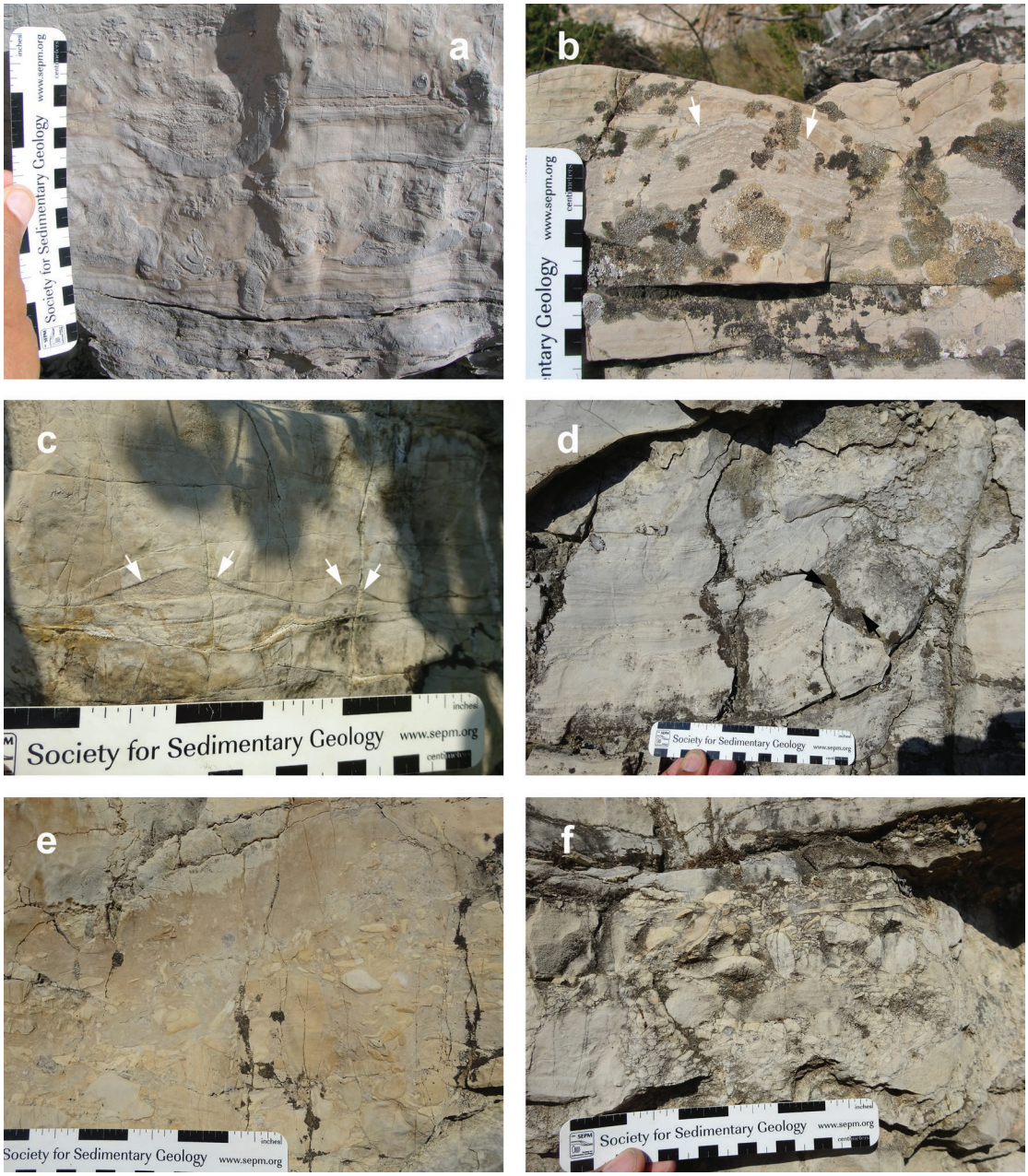

Fig. 5. Dolomites in the Opletnya Member: **a** — dolo-wackestone with chaotic soft-sediment deformation and subsequent bioturbation, Lakatnik section, 82.90 m, elementary sequence 42; **b** — dome-shape stromatolite (below arrows), developed in the uppermost part of the fourth medium-scale sequence, Lakatnik section, 110.3 m, elementary sequence 60; **c** — symmetric small ripples of packstone (arrows), surrounded by mud- to wackstone in a dolomitized bed-set. Sfrazen section, 109.5 m, elementary sequence 60; **d** — tepee structure from the upper part of small-scale sequence 12, Sfrazen section, 49.1 m, elementary sequence 23; **e** — matrix-supported floatstone rich in pebble-sized, subrounded intraclasts, Sfrazen section, 49.3 m, elementary sequence 24; **f** — clast-supported lag deposit of conglomerate, Sfrazen section, same level as (e). The position in meters refers to the base of the Opletnya Member, the elementary and small-scale sequence numbering is according to Fig. 7.

Synsedimentary deformation, some of it with sigmoidal geometry, is among the often observed features in wacke- and mudstones (Figs. 6a, 7), and beds with this texture are common in the lower part of the Opletnya Member. Its amplitude commonly is in the range of 5–15 cm, but in some beds may reach or even exceed 40 cm. Several internally deformed beds may be vertically stacked (Fig. 6b). The upper bounding surface of the deformation structures may be flat but more often is slightly concave-up. These structures can be traced laterally over several tens of meters, whereby their amplitude gradually decreases and finally disappears (Fig. 6d). Small- and meso-scale slump folding is another type of synsedimentary deformation common in wacke- and mudstones, observed in almost the whole Opletnya Member. In some places, direct contact between sigmoidal and slump folding structures can be observed (Fig. 6c). The geometry of these structures varies

from quite symmetrical folding (Fig. 6f) to chaotic (Fig. 5a). Most commonly these slump folds have amplitudes in the range of 30 to 50 cm, but in some cases may exceed 2 m (Fig. 6e). These features are interpreted as having formed by sliding of soft but cohesive sediment, possibly by instabilities on channel margins (Hardie & Garrett 1977), or induced by the occasional impact of storm waves or earthquakes (seismites; Montenat et al. 2007).

Although wacke- and mudstones are common in the studied sections, this lithology is dominant in the lower part of the Opletnya Member. Mudstones mark the deepest and/or most quiet sedimentary environments, with restricted water circulation. The intense bioturbation supports this interpretation. The nodularity often is connected with increased clay content as a result of increased terrigenous supply.

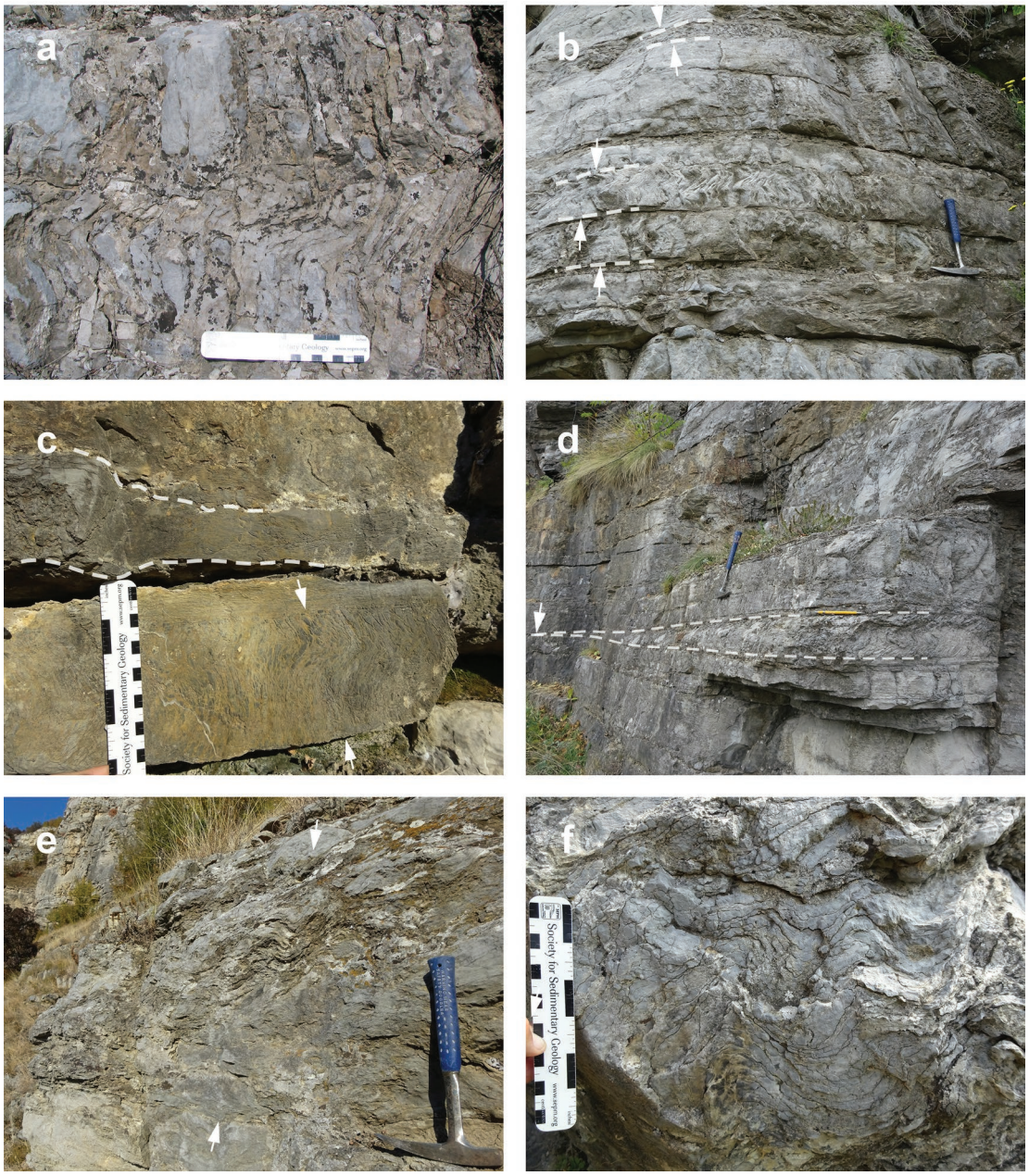

Fig. 6. Synsedimentary deformations in the Opletnya Member: **a** — 40 cm thick bed with sigmoidal structure from the middle part of the medium-scale sequence, Lakatnik section, 15.3 m, elementary sequence 7; **b** — two stacked beds (between dashed lines and arrows) with sigmoidal structure and another one above them. Sfrazen section, 13.1 m, elementary sequence 6; **c** — wackestone bed with sigmoidal structure (between arrows) overlain by a mudstone bed (between dashed lines) with slumps, Sfrazen section, 24.1 m, elementary sequence 12; **d** — 12 cm thick bed with sigmoidal structure (between dashed lines) with concave top surface that pinches out laterally (arrow). Hammer for scale, Lakatnik section, 12.0 m, elementary sequence 6; **e** — about 2 m thick wacke- to mudstone bed with slumps (between arrows) in its lower part (hammer for scale), Sfrazen section, 28.2 m, elementary sequence 14; **f** — detail of the same level shown in (e). The position in meters is from the base of the Opletnya Member, the elementary sequence numbering is according to Fig. 7.

Packstones, grainstones, rudstones, and floatstones

Bioclasts, mudstone lithoclasts, ooids as well as a high amount of peloids are the typical components of the pack- and grainstones. Rudstones and floatstones are very rare; they contain pebble- to cobble-sized intraclasts, the roundness of which varies in a wide range. The intraclasts are either chaotically distributed (Fig. 4e), or they occur in the bottom set (Fig. 4f) or on the foreset surfaces of cross-beds (Fig. 4d). Lag deposits and imbrication structures are also observed. In some cases, the surfaces of the intraclasts are not sharp and show a gradual transition to the hosting material, which could be the result of re-sedimentation of semi-lithified material, or incipient disintegration of the semi-consolidated beds (Fig. 4e). Some beds are strongly bioturbated (Fig. 4f) and may show overpacking due to early compaction. Partial dolomitization is more common in packstones than in grainstones.

Packstones, grainstones, and rudstones/floatstones commonly form massive beds. The most prominent sedimentary structure is the well-developed cross-bedding — low-angle, planar and trough type — commonly with thick lamination (Fig. 4c,d,f). Small-scale cross-bedding displays both wavy bedding (Fig. 5c) and current ripples (Fig. 4d). Reactivation surfaces are also common (Fig. 4d). The set thickness ranges between a few cm to a few tens of cm, while that of the cosets may reach several meters (Fig. 7). Such sediment bodies can form regionally traceable bed packages, which have been considered as stratigraphic markers (Tronkov 1968). The cross-bedding direction varies in a wide range — within one coset as well as along the same level in both sections (Fig. 7).

The pack- and grainstone beds indicate an active hydrodynamic sedimentary environment that led to the development and lateral migration of different types of bars and shoals. The variety of morphology, scale, and orientation of the cross-bedding, the reactivation and accretion surfaces, and the intercalation of these features indicate highly variable high-energy settings typical of shallow-water environments. The presence of intraclasts, some of them semi-lithified, implies an almost permanent subaqueous erosion by waves and currents. Wavy bedding and the variable orientation of the cross-beds suggest a tidal influence (e.g., Reineck & Singh 1975; Gonzales & Eberli 1997).

Dolomites

The partially or completely dolomitized packstones, wackestones, and mudstones have an uneven distribution in the studied sections. They can be observed as thin to thick beds, but may also stack into packages with thicknesses of 2.65–2.80 m or even 3.25–3.55 m that intercalate with several very thin beds of mixed carbonate-terrigenous rocks (Fig. 7). In the middle and upper parts of the Opletnya Member, almost completely dolomitized sets of 9.50 to 14.80 m can be observed. Although massive and laminated structures are most common for these rocks, they also are associated with tepees and flat pebbles that form local lags (Fig. 5d). Nodular structures are also present. Lenses with chaotically oriented lithoclasts (Fig. 5e,f), some of them with imbrication structures, are common. In some beds, most often dolo-packstones and rare dolo-grainstones, different types of cross-bedding can be observed (Fig. 5c), and intraclasts may form short bands lying on the foreset lamina. Stromatolites with different morphologies, developed in dolomitized mud- and wackestone beds, are observed at several levels in the studied sections (Figs. 5b, 7).

The dolomite-dominated intervals are interpreted as the shallowest, high-salinity sedimentary environment in the Opletnya Member. Desiccation cracks and tepee structures mark episodes of subaerial exposure, indicating the establishment of tidal flats under a semi-arid climate. These climatic conditions are favorable for microbially-mediated dolomitizaton of microbial mats (e.g., Petrash et al. 2017) and/or early-diagenetic reflux dolomitization (e.g., Adams et al. 2018). However, no detailed geochemical studies were preformed and the possibility of late-diagenetic dolomitization cannot be excluded either (e.g., Lukoczki et al. 2019). Storm events and/or strong tidal currents ripped up cohesive sediment, incipient hardgrounds, or microbial mats to form flat-pebble conglomerates and lag deposits (e.g., Hardie & Ginsburg 1977; Hillgärtner et al. 2002).

Erosion surfaces

Other common features of the Opletnya Member are the erosional surfaces. Often they demonstrate channel morphology (Fig. 8a–c). In many cases, the flanks of these channels are very steep to almost vertical, indicating a relatively advanced degree of cohesion and early lithification of the sediment into which the channel was cut (Fig. 8b). The erosion surfaces either separate beds of different lithology (Fig. 8a,b and d), or they occur within a set of lithologically monotonous beds and are underlain by thin layers or lenses of mixed siliciclastic–carbonate or fully siliciclastic material (Fig. 8c). Stacking of multiple erosional surfaces is documented at several levels of the profile. The erosional depth varies between 5–15 cm and several tens of centimeters, but in some cases reaches even 60–80 cm (Figs. 7 and 8a). Lag deposits draping the erosional surfaces are observed in some cases.

Firmgrounds and hardgrounds

Firm- and hardgrounds on top of dolomitic limestone and dolomite beds are also observed (Figs. 7 and 8d). They are irregular, with amplitudes of several centimeters. Borings belong to *Balanoglossites* and *Trypanites*, characteristic ichnotaxa of Middle Triassic ramp settings (Knaust 1998, 2007; Knaust et al. 2012; Chrząstek 2013).

Lakatnik Member

Limestones, thick-bedded pack- and grainstones, are also dominant in the Lakatnik Member (upper Mogila Formation). This member is furthermore characterized by levels rich in

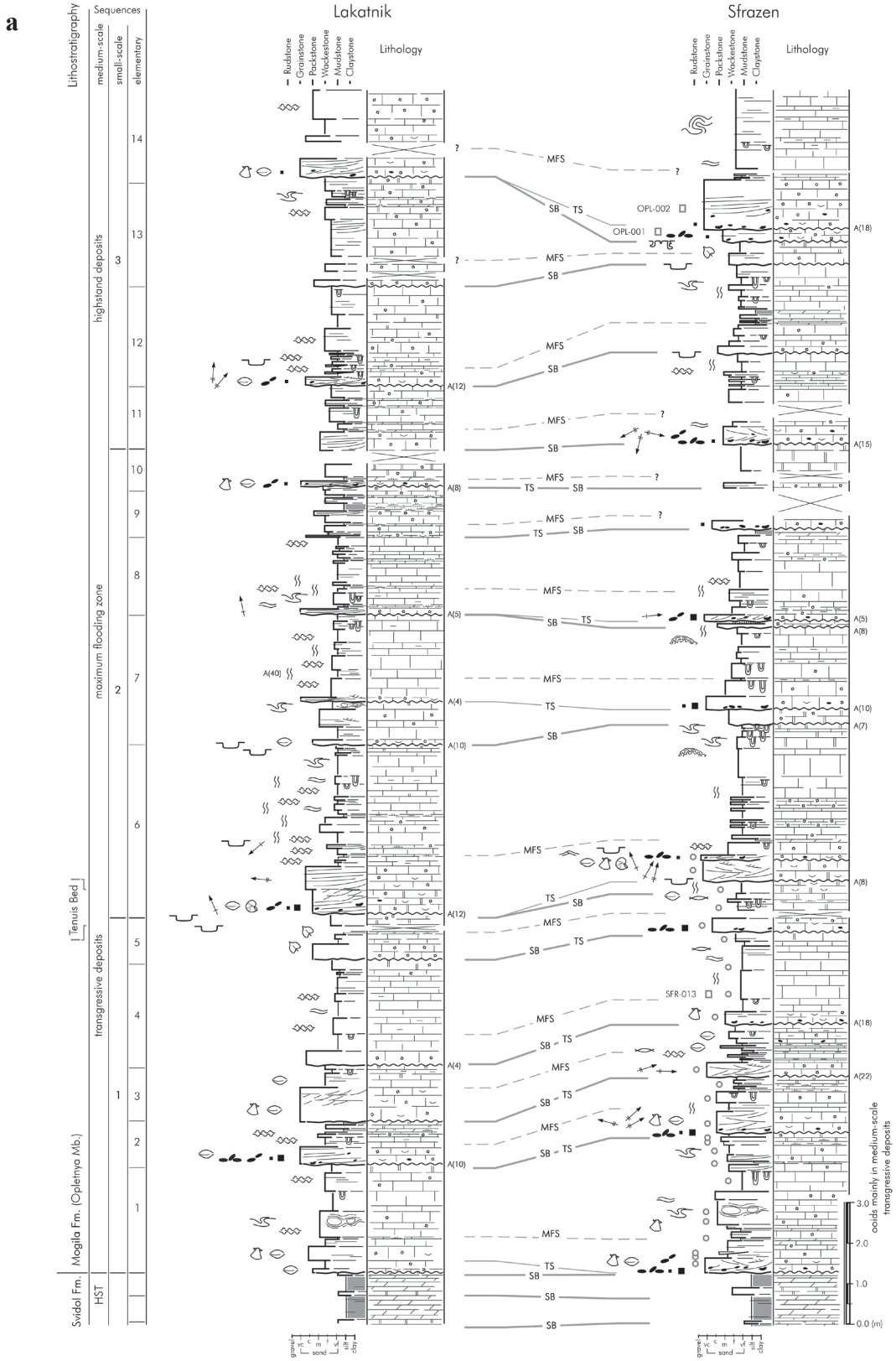

Fig. 7. Sequence- and cyclostratigraphic interpretation of the Opletnya Member (Mogila Formation) in the Lakatnik and Sfrazen sections: **a** — lowermost part of the Opletnya Member (including the Tenuis Bed); **b** — lower part of the Opletnya Member (including the Zitolub Bed); **c** — middle part of the Opletnya Member (including the Sfrazen Bed); **d** — upper part of the Opletnya Member (including the Sedmochislenitsi Bed and the prominent Anisian sequence boundary An1); **e** — uppermost part of the Opletnya Member (top Sedmochislenitsi Bed to the boundary between the Opletnya and Lakatnik members). The maximum amplitude (A, in cm) is indicated for the prominent erosional surfaces. SB: sequence boundary; TS: transgressive surface; MFS: maximum-flooding surface.

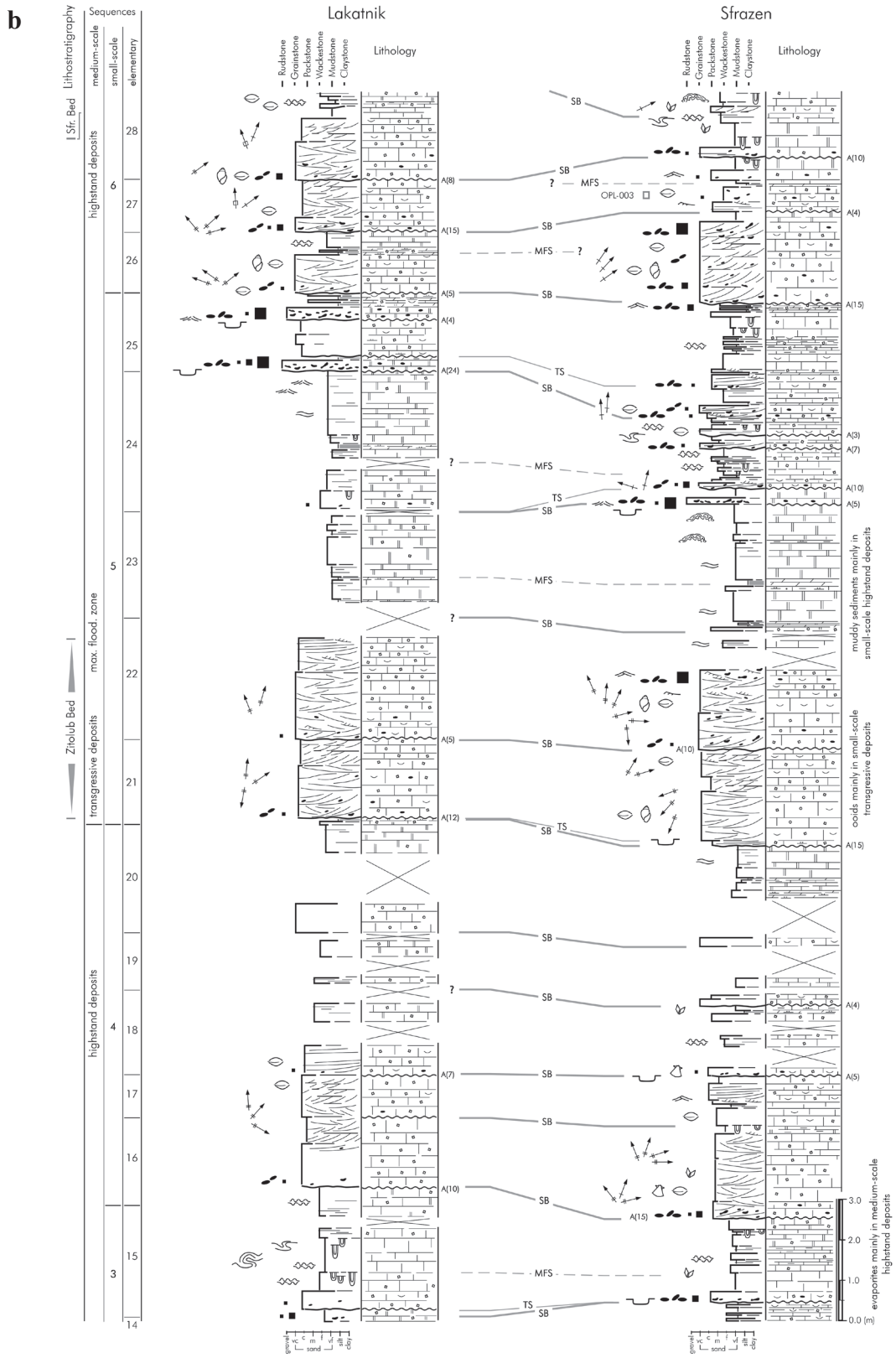

Fig. 7. (continued) Sequence- and cyclostratigraphic interpretation of the Opletnya Member (Mogila Formation) in the Lakatnik and Sfrazen sections: **a** — lowermost part of the Opletnya Member (including the Tenuis Bed); **b** — lower part of the Opletnya Member (including the Zitolub Bed); **c** — middle part of the Opletnya Member (including the Sfrazen Bed); **d** — upper part of the Opletnya Member (including the Sedmochislenitsi Bed and the prominent Anisian sequence boundary An1); **e** — uppermost part of the Opletnya Member (top Sedmochislenitsi Bed to the boundary between the Opletnya and Lakatnik members). The maximum amplitude (A, in cm) is indicated for the prominent erosional surfaces. SB: sequence boundary; TS: transgressive surface; MFS: maximum-flooding surface.

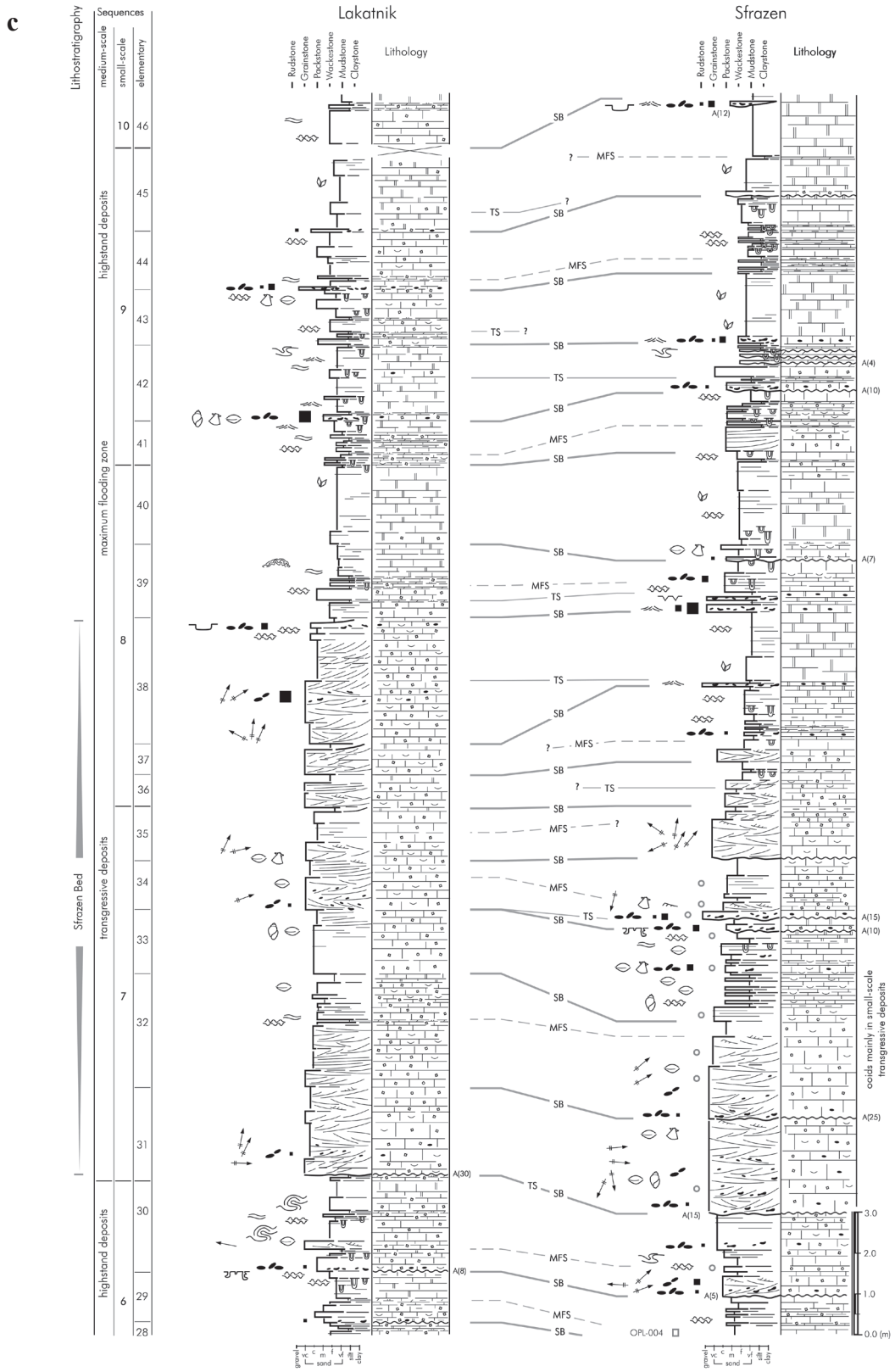

Fig. 7. (continued) Sequence- and cyclostratigraphic interpretation of the Opletnya Member (Mogila Formation) in the Lakatnik and Sfrazen sections: **a** — lowermost part of the Opletnya Member (including the Tenuis Bed); **b** — lower part of the Opletnya Member (including the Zitolub Bed); **c** — middle part of the Opletnya Member (including the Sfrazen Bed); **d** — upper part of the Opletnya Member (including the Sedmochislenitsi Bed and the prominent Anisian sequence boundary An1); **e** — uppermost part of the Opletnya Member (top Sedmochislenitsi Bed to the boundary between the Opletnya and Lakatnik members). The maximum amplitude (A, in cm) is indicated for the prominent erosional surfaces. SB: sequence boundary; TS: transgressive surface; MFS: maximum-flooding surface.

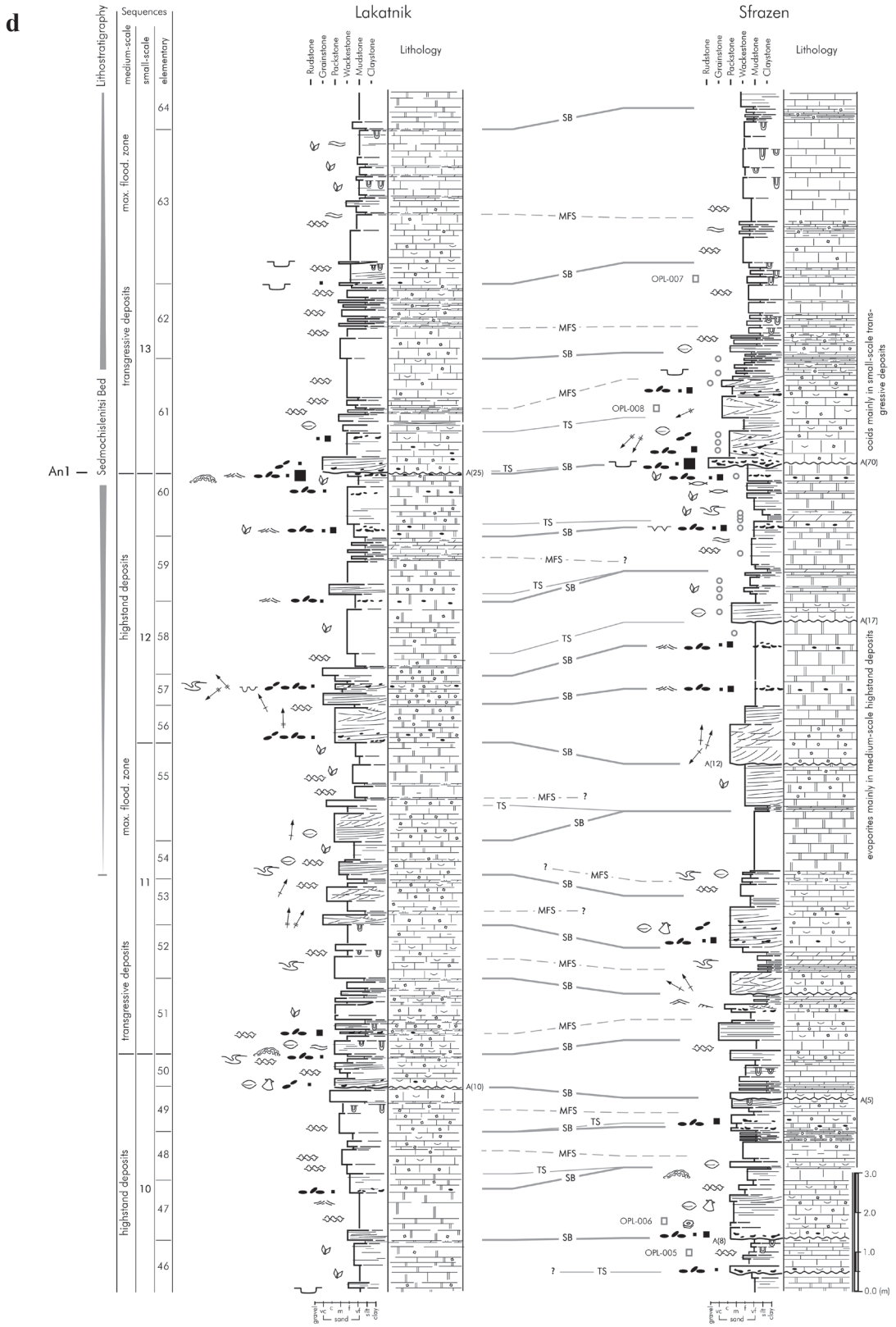

Fig. 7. (continued) Sequence- and cyclostratigraphic interpretation of the Opletnya Member (Mogila Formation) in the Lakatnik and Sfrazen sections: **a** — lowermost part of the Opletnya Member (including the Tenuis Bed); **b** — lower part of the Opletnya Member (including the Zitolub Bed); **c** — middle part of the Opletnya Member (including the Sfrazen Bed); **d** — upper part of the Opletnya Member (including the Sedmochislenitsi Bed and the prominent Anisian sequence boundary An1); **e** — uppermost part of the Opletnya Member (top Sedmochislenitsi Bed to the boundary between the Opletnya and Lakatnik members). The maximum amplitude (A, in cm) is indicated for the prominent erosional surfaces. SB: sequence boundary; TS: transgressive surface; MFS: maximum-flooding surface.

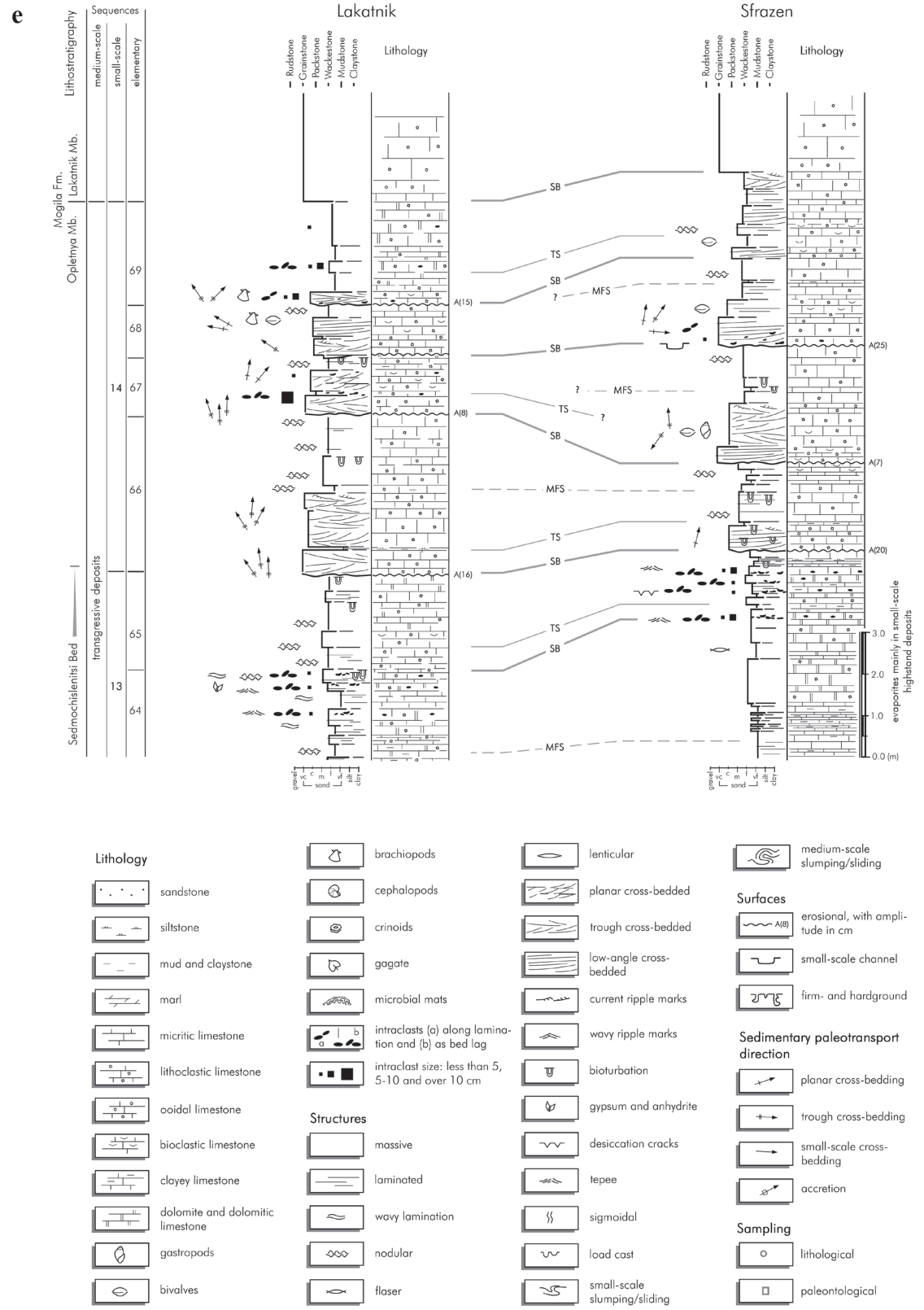

Fig. 7. (continued) Sequence- and cyclostratigraphic interpretation of the Opletnya Member (Mogila Formation) in the Lakatnik and Sfrazen sections: **a** — lowermost part of the Opletnya Member (including the Tenuis Bed); **b** — lower part of the Opletnya Member (including the Zitolub Bed); **c** — middle part of the Opletnya Member (including the Sfrazen Bed); **d** — upper part of the Opletnya Member (including the Sedmochislenitsi Bed and the prominent Anisian sequence boundary An1); **e** — uppermost part of the Opletnya Member (top Sedmochislenitsi Bed to the boundary between the Opletnya and Lakatnik members). The maximum amplitude (A, in cm) is indicated for the prominent erosional surfaces. SB: sequence boundary; TS: transgressive surface; MFS: maximum-flooding surface.

crinoids. Lenses of dolomitic limestones and dolomites are intercalated.

Babino Formation

The lower part of the Babino Formation (Zimevitsa Member) is dominated by nodular, clayey, rare massive and laminated, often bioturbated wacke- to mudstones (Fig. 9c) that alternate with mainly bioclastic, massive to cross-bedded packstones (Fig. 9a,b,d). Along the base of the unit, as well as in several distinct beds above, levels rich in brachiopods and crinoids are observed (Figs. 9b,d, 10). The volume of mixed siliciclastic-carbonate rocks is minor. Synsedimentary deformation structures are common. At around 10 m from the base of the unit, an erosional, karstified surface with evidence for subaerial exposure is observed (Fig. 9a). The upper half of the Babino Formation (Zgorigrad Member) is formed by mainly nodular, thin- to medium-bedded wacke- and packstones that contain conodonts, bivalves, and brachiopods.

The Babino Formation is covered by the massive to thick-bedded dolomites with crinoids of the Milanovo Formation.

Sequence stratigraphy and cyclostratigraphy

Concepts

The sequence- and cyclostratigraphic interpretation and the correlation of the studied sections follow the concepts proposed by Strasser et al. (1999). The sequence-stratigraphic nomenclature is that of Catuneanu et al. (2009), and this nomenclature is applied independent of the scale of the sequences (Posamentier et al. 1992; Catuneanu 2019). Sequence boundaries (SB) are indicated by the shallowest facies and may in addition be expressed by an erosive surface if sea level dropped below the previously accumulated sediment. Transgressive surfaces (TS) may be erosive if there was ravinement, and in any case mark the beginning of a deepening-up facies trend (transgressive deposits). Maximum-flooding surfaces (MFS) are expressed by the deepest facies and display bioturbation or hardgrounds if sedimentation rate was reduced. Shallowing-up highstand deposits then lead to the following sequence boundary.

Elementary sequences are the smallest units in which facies trends and sedimentary structures indicate a cycle of sea-level

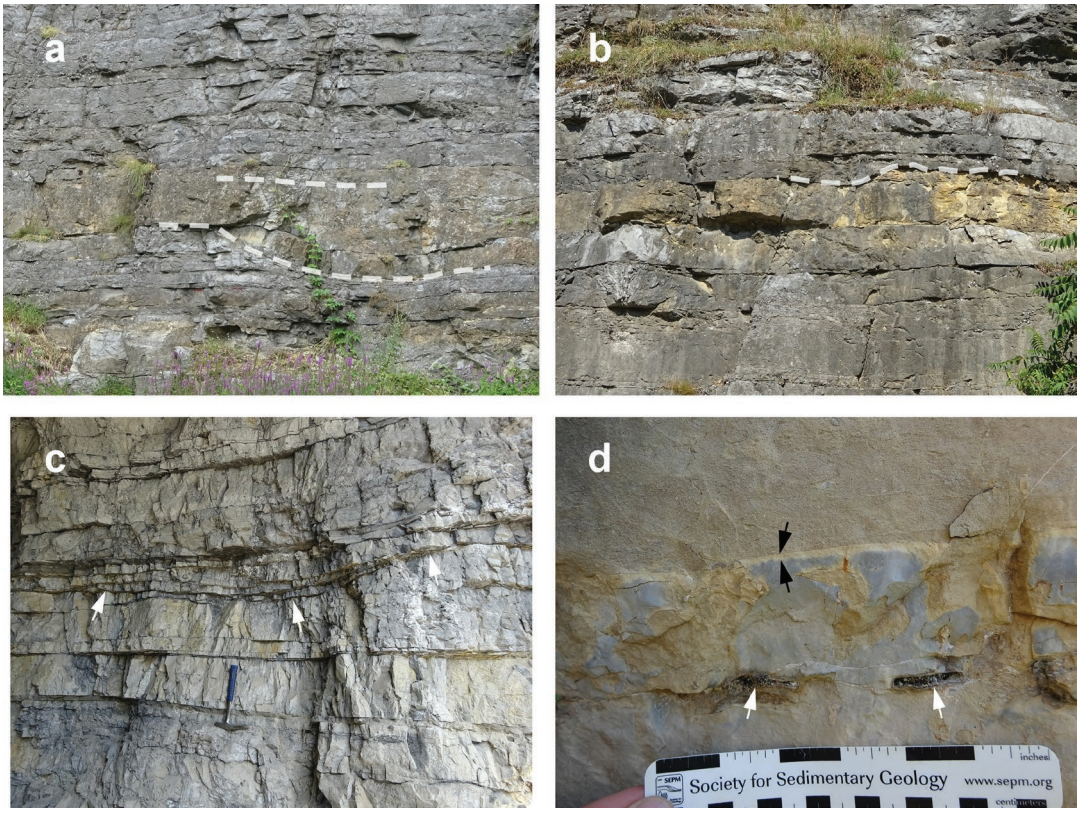

Fig. 8. Erosional surfaces in the Opletnya Member: **a** — two erosional surfaces (dashed lines), partly developed in dolomitized limestone, the lower one forming a channel over 50 cm deep that marks a sequence boundary, Lakatnik section, 9.2 m, elementary sequence 6; **b** — small-scale channel with steep flanks (dashed line), filled by limestones developed in the uppermost part of dolomites. The channel is 12 cm deep, Lakatnik section, 14.2 m, elementary sequence 7; **c** — small-scale channel (hammer for scale) that laterally corresponds to a level with sigmoidal synsedimentary deformation, Lakatnik section, 11.9 m, elementary sequence 6; **d** — hardground surface at the top of highstand dolomitic limestones (black arrows), covered by bioclastic grainstones. The highstand deposits contain gagate intraclasts (above white arrows). The top of the bed appears broken, with reddish sediment infill, Sfrazen section, 25.4 m, elementary sequence 13. The position in meters refers to the base of the Opletnya Member, the elementary sequence numbering is according to Fig. 7.

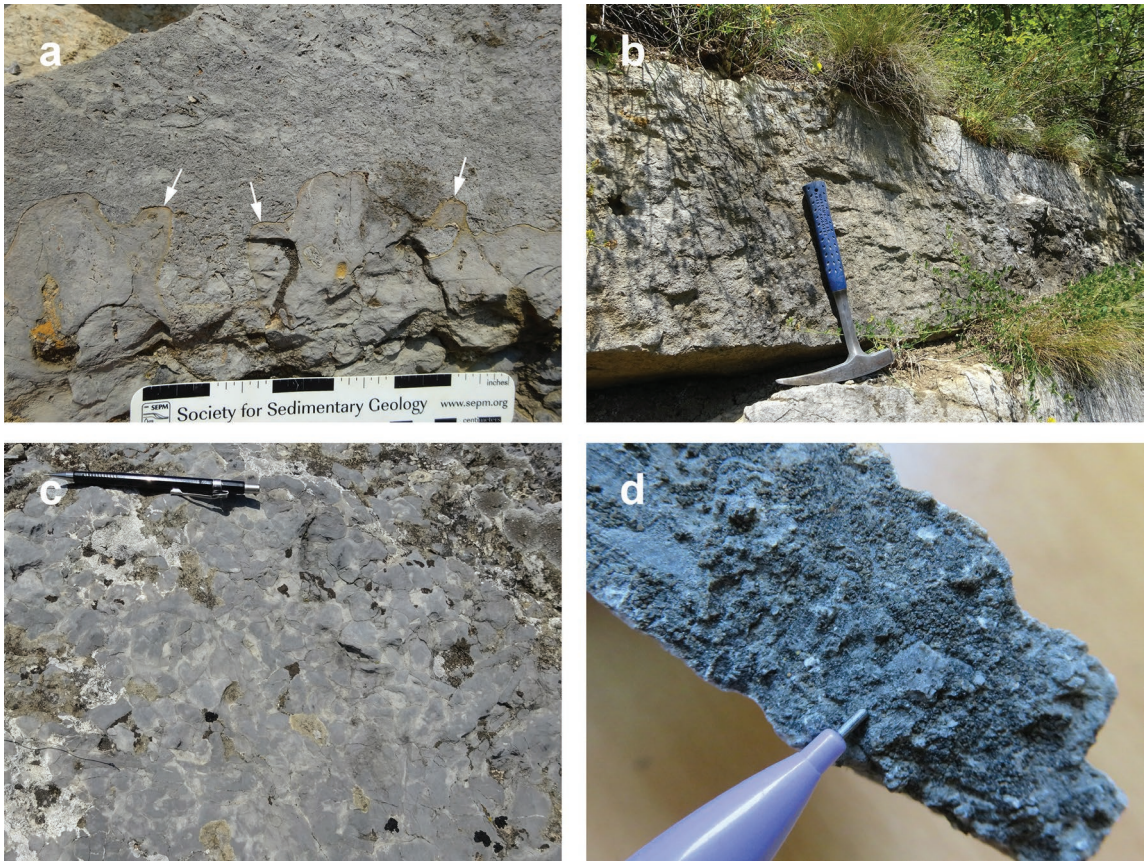

Fig. 9. Lithology of the lower Zimevitsa Member (lower Babino Formation) in the Sfrazen section: **a** — highly irregular paleokarst surface (arrows) implying prolonged subaerial exposure, overlain by bioclastic limestone; **b** — low-angle cross-bedded limestone, transgressive deposits of an elementary sequence; **c** — plan view of nodular wackestone from the middle part of an elementary sequence; **d** — crinoid columnal segment of *Holocrinus dubius* from transgressive deposits in the lower part of the Zimevitsa Member. All photos are from elementary sequence 6 in Fig. 10.

change. Small-scale sequences are composed of several (in many cases five) elementary sequences and generally display first a deepening then a shallowing trend, with the shallowest facies at the boundaries. Several (2 to 4 in the studied sections) small-scale sequences compose a medium-scale sequence, which again displays a general deepening-shallowing trend of facies evolution and the relatively shallowest facies at its boundaries. If several elementary sequences compose an interval of shallowest or deepest facies, a sequence-boundary zone respectively a maximum-flooding zone is defined (Montañez & Osleger 1993).

Small, meter-scale depositional units are often called "cycles" if they are stacked in the sedimentary record. Here we use the term "sequence" because this allows better defining the facies evolution within them and interpreting the sea-level changes that caused it. If such sequences are bounded by prominent marine flooding surfaces, they can be compared to the "parasequences" of van Wagoner et al. (1990), although these were originally defined in siliciclastic systems. We use the term "cycle" for the cyclical or periodic processes that controlled the formation of the sequences.

If chronostratigraphic tie points allow estimating the duration of the studied sections, and if the hierarchical stacking of the depositional sequences reflects the ratios of orbital (Milankovitch) cyclicity, an interpretation of the evolution of the depositional environments can be proposed at a high time resolution: the elementary sequences would correspond to the 20-kyr precession cycle, the small-scale sequences to the 100-kyr short eccentricity cycle, and the medium-scale sequences to the 405-kyr long eccentricity cycle. These orbital cycles translated into sea-level cycles through complex atmospheric and oceanic feed-back processes (Strasser 2018). However, autocyclic processes independent of orbital cycles may have been superimposed, making the interpretation more complicated. Time-series analyses are commonly applied to demonstrate the recording of orbital cyclicity (e.g., Hinnov 2013). In the present case, however, the complexity of the facies changes on the shallow ramp precludes such an approach.

Elementary sequences

In both studied sections of the Opletnya Member (lower part of the Mogila Formation), 69 elementary sequences were identified and correlated (Fig. 7). These are generally grouped by five to form 14 small-scale sequences. Two or four small-scale sequences are bundled into 5 medium-scale sequences,

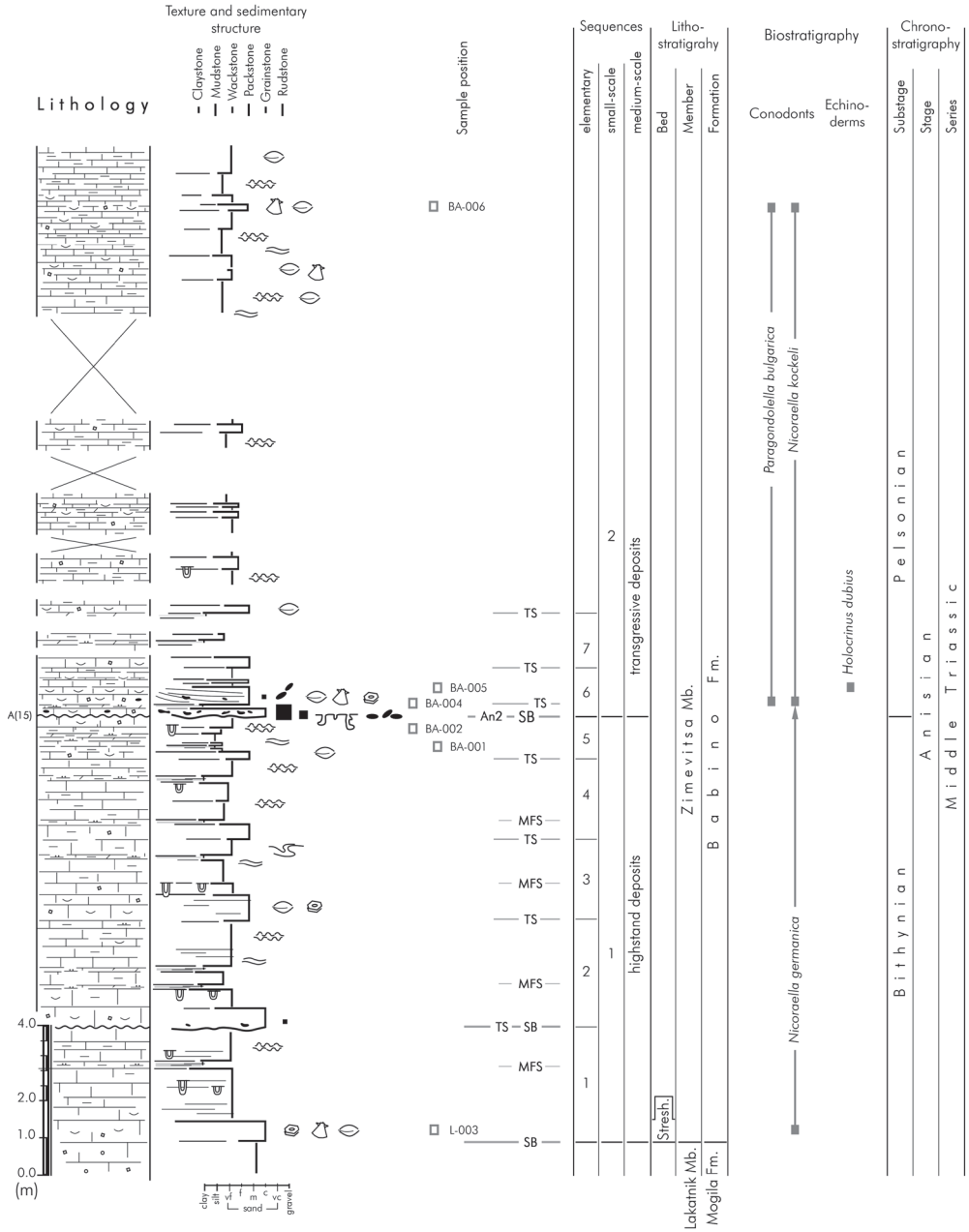

Fig. 10. Cyclostratigraphic interpretation of the lower Babino Formation (Zimevitsa Member), Sfrazen section. The legend is according to Fig. 7.

in which three parts can be recognized: transgressive, maximum-flooding, and highstand deposits. Elementary and small-scale sequences are recognized also in the lowermost part of the Zimevitsa Member (lower part of the Babino Formation).

The elementary sequences, the smallest cyclic units documented, are defined by their bounding surfaces, composition, facies trends, and sedimentary structures that indicate a cycle of sea-level change. The base of each elementary sequence is marked by the shallowest facies, and/or by a laterally traceable erosional surface. Most of the elementary sequences can be subdivided into three parts — a lower part that represents the transgressive stage, a middle part containing the maximum-flooding surface, and an upper part representing the highstand stage. The facies composition and thickness of these parts varies depending on the position of the elementary sequence within the small-scale and especially the medium-scale sequence it belongs to (Strasser et al. 1999).

In the lower (transgressive) part of a medium-scale sequence, the sequence boundary and the transgressive surface of the elementary sequences are very close to each other or even amalgamated because lowstand deposits are very thin or not recorded due to limited accommodation on the shallow ramp (Fig. 11). Intraclasts, lithologically identical to the rocks immediately below the erosional surface, indicate reworking during transgression of previously cemented sediment. Massive or cross-bedded pack- and grainstones represent

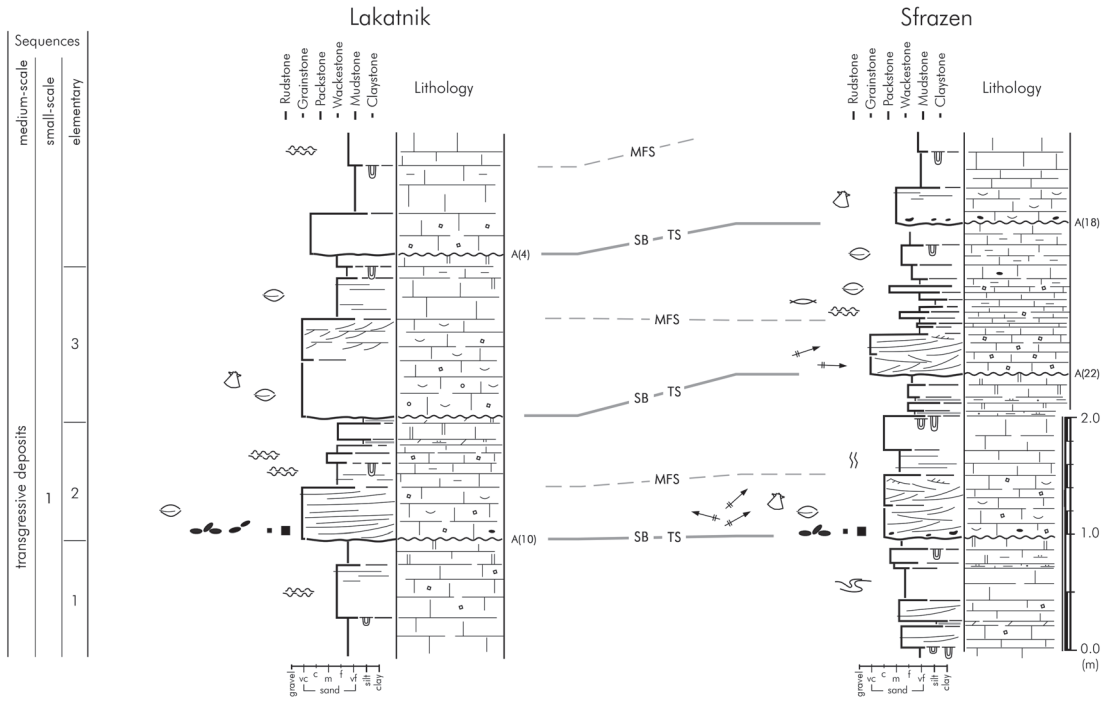

Fig. 11. Elementary sequences from the transgressive part of the lowermost medium-scale sequences of the Opletnya Member. Note that SB and TS are amalgamated and represent a ravinement surface. Elementary and small-scale sequence numbering and legend as in Fig. 7.

shallow bars or shoals that formed during transgression, and they may form 30–50 % of the volume of the elementary sequences. The maximum-flooding surface marks the top of these beds or can be identified above by the deepest facies and/or intense bioturbation. In the early highstand part of these elementary sequences, massive, laminated or nodular, often bioturbated wacke- and mudstones dominate. The amount of terrigenous components increases and forms thin beds of marls or of mixed siliciclastic-carbonate sediment. In some cases, the uppermost, late highstand part is dolomitic limestone or (rarely) dolomite (Fig. 11). In other cases, the late highstand is formed by marly wacke- and mudstone beds.

In the studied sections, the average thickness of the elementary sequences from the transgressive part of the medium-scale sequences is in range of 2.1–2.2 m. The thickest elementary sequences (3.9 to 4.25 m) are measured in the lowermost and uppermost medium-scale sequences of the Opletnya Member (Fig. 7). A gradual but steady decreasing in the average thickness (from 2.3 to 1.5 m) of the elementary sequences is observed in the transgressive part of the first four medium-scale sequences.

In the maximum-flooding to early highstand parts of the medium-scale sequences, the elementary sequences are dominated by wacke- and mudstones while pack- and grainstones occur in lesser amounts (Fig. 12). Once again, the pack- and grainstone beds occupy mainly the base of these units and rarely occupy the whole transgressive part, where the amount of the wacke- and mudstone gradually increases. Intraclasts are rare and small in size. The transgressive surface of these elementary sequences can be very close to the sequence boundary or coincides with it. However, at the top of elementary sequence 7 in the Sfrazen section, the lower erosion surface is interpreted as the sequence boundary, while the second erosion surface represents the transgressive (ravinement) surface. Thus, a thin lowstand deposit is present. The maximum-flooding surface is associated with increasing intensity of bioturbation and, in some cases, synsedimentary deformation. The highstand interval, dominated by massive or laminated mud- and wackestones, forms 70–80 % of the elementary sequences. Dolomitization of their uppermost part is rare. However, sediment containing terrigenous siliciclastics forms thicker and laterally traceable units.

In the highstand parts of the medium-scale sequences, the transgressive deposits of the elementary sequences are represented by pack- and grainstones, and/or by mixed siliciclastic–carbonate or even claystone beds (Fig. 13). Dolomite and dolomitic limestones are common. The sequence boundary is represented by desiccation cracks, tepee structures, or an erosional surface. The transgressive surface, where it can be identified, is above the sequence boundary, making room for thin lowstand deposits. The maximum-flooding surface cannot always be recognized. Wacke- and mudstones dominate the upper part of the units. In many of these elementary sequences, almost the whole volume is represented by dolomite or partially dolomitized limestones.

The average thickness of the elementary sequences within the highstand parts of medium-scale sequences is around 2.05 m. This value decreases in the lower (early) stage of the highstand part to 1.3–1.5 m, while in the upper (late) part it increases to 1.8–1.9 m.

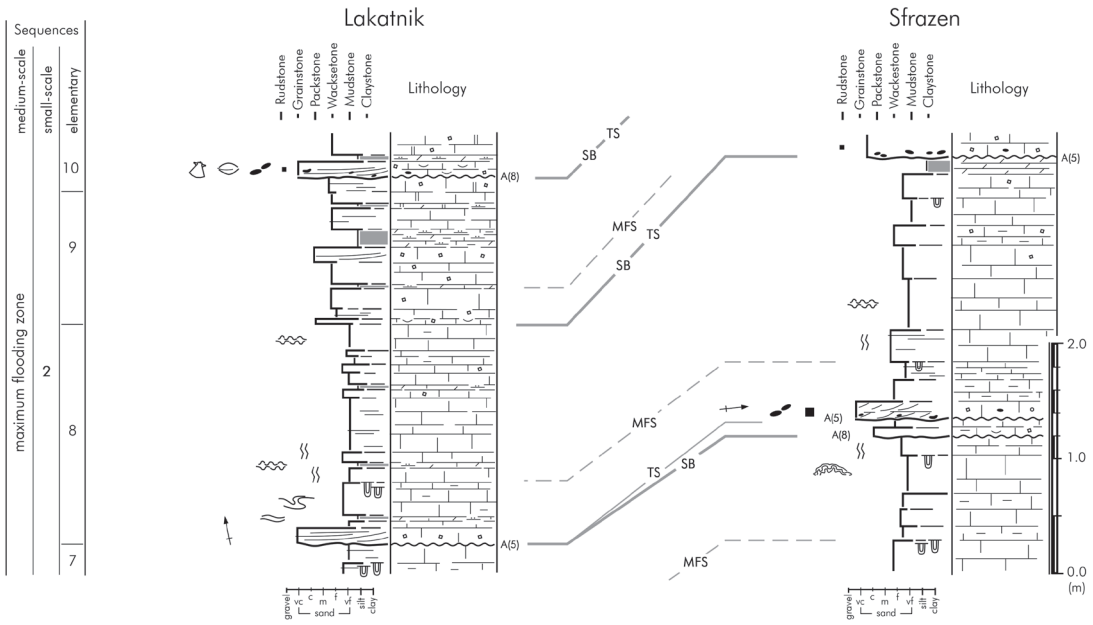

Fig. 12. Elementary sequences in the maximum-flooding zone of the lowermost medium-scale sequence of the Opletnya Member. Elementary and small-scale sequence numbering and legend as in Fig. 7.

In the Lakatnik Member, it is not possible to clearly define elementary sequences. In the lowermost part of the Zimevitsa Member (Babino Formation), the elementary sequences are less complex than those in the Opletnya Member. Their base is marked by a transgressive surface (Fig. 10). Erosional surfaces are rare. The sequence boundaries generally are not developed (elementary sequences defined by transgressive surfaces; Strasser et al. 1999), with the exception of the ones at the base of elementary sequences 2 and 6. The transgressive part is presented by massive, laminated to low-angle cross-bedded bio- and lithoclastic pack- to grainstones (Fig. 9b). Terrigenous fines increase from the maximum-flooding surface into the highstand part of the units, where massive, laminated and nodular wacke- and mudstones predominate (Fig. 9c). Bioturbation is very common. The average thickness of the elementary sequences is similar to that in the Opletnya Member and is in the range of 2–2.2 m.

Small-scale sequences

Within the Opletnya Member, the elementary sequences, grouped into sets of five, form a succession of 14 small-scale sequences (Fig. 7). Their base very often is marked by a pronounced erosional surface and/or a lag of intraclasts. The measured erosional amplitude of these surfaces ranges from a few centimeters to decimeters and, in individual cases such as at the limit between small-scale sequences 12 and 13 in the Sfrazen section, may reach more than 70 cm (Figs. 7d and 13). Stacking of several erosional surfaces within one elementary sequence situated at the base of the small-scale sequences is also common (Figs. 4f, 8a). Similar erosional stacking can be observed along the boundary between the first two elementary sequences in the second small-scale sequence (Fig. 8b).

From the base upwards, the small-scale sequences display first a deepening then a shallowing trend. The boundary between them is always marked by the shallowest facies. Most commonly, their lower part is dominated by limestones and/or partially dolomitized limestones — litho- and bioclastic or ooid-dominated pack- and/or grainstones (Figs. 4e,f, 7, 8a). Massive, planar and trough cross-bedding with lags of intraclasts is common (Fig. 4c). Reactivation and lateral accretion surfaces are observed. Different types of small-scale cross-bedding, indicating wave or current hydrodynamic regimes, are also typical for this part. The paleotransport directions vary in a wide range and in one and the same elementary sequence almost opposite directions can be observed (elementary sequences 21, 22, and 31 in Fig. 7b,c).

Upsection, the thickness of the pack- and grainstones in the small-scale sequences decreases and the amount of wackestone beds increases, marking a deepening facies trend. The amount of nodular and finely laminated beds increases. Also, a gradual increase in frequency and intensity of bioturbations is observed (Figs. 4a, 5a). The evidences for erosional processes gradually decrease. Firm- and hardground surfaces are developed (Figs. 7, 8d).

The turn-around to a shallowing facies trend is marked by the gradual increase of the amount of terrigenous material and dolomite, of the frequency of erosional features, and of synsedimentary deformations (for example small-scale sequences 2, 5, 6, 8 and 12 in Fig. 7). In many cases, the amount of packstone beds also increases. At such turning points, in the lower part of the Opletnya Member, the maximum bed thickness (40 cm) with sigmoidal structures is recorded. Commonly, the shallowing-upwards trend is accompanied by an increase in erosional and synsedimentary deformation structures, forming in some places a stacked pattern (Fig. 6e,f; Fig. 7b: elementary

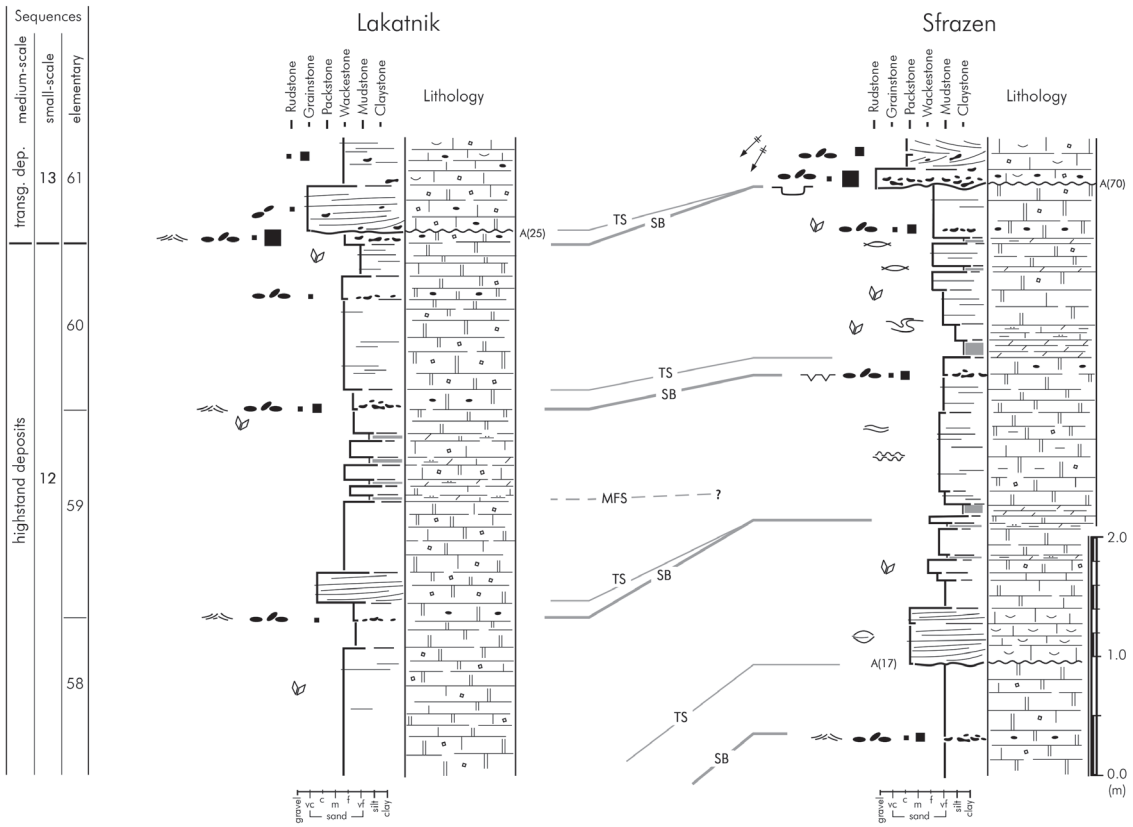

Fig. 13. Elementary sequences from the highstand part of the fourth medium-scale sequence of the Opletnya Member. Elementary and small-scale sequence numbering and legend as in Fig. 7.

sequence 25). Laterally, the intensity of these features may change rapidly: while in one section they are quite prominent, in the other they are attenuated (e.g., elementary sequences 14, 15, and 30 in Fig. 7a,b,c). In dolomite-dominated small-scale sequences, different types of lag deposits (Fig. 5e,f) are commonly associated with tepees (Fig. 5d) and desiccation cracks. In this shallowing part, the finely laminated and nodular structures still dominate (Fig. 4b), but small-scale cross-bedding also is common (Figs. 4d, 5c).

The pattern described above varies within the studied sections. For example, bioclastic to intraclastic packstones may predominate almost entirely in one small-scale sequence (Fig. 7c: small-scale sequence 7) while in other cases (Fig. 7c,d: small-scale sequences 9 and 12) the dolomitic lithology is more prominent.

The thickness of the small-scale sequences within the Opletnya Member varies in the range of 6.7–14.4 m (average 9.6 m). Only in small-scale sequences 3, 5, and 13, the thickness is over 11 m (Fig. 7a,b,d,e). Depending on to which part of a medium-scale sequence the small-scale sequences belong to, a persistent trend in the thickness of the elementary sequences is observed. For example, within the transgressive part of the medium-scale sequences, the small-scale sequences demonstrate a symmetrical pattern with the thinnest elementary sequences in the middle (Fig. 7). Around the maximum-flooding and early highstand part of the medium-scale sequences, the thickness of the elementary sequences within the small-scale sequences decreases, while in their late highstand parts of the medium-scale sequences the small-scale sequences contain thicker elementary sequences in their upper part (for example small-scale sequence 8; Fig. 7c).

One small-scale sequence, bounded by erosional surfaces, was identified in the lowermost Babino Formation (Zimevitsa Member). The thickness of the elementary sequences within it decreases upwards from 3.3 m to 1.15 m (Fig. 10). The total thickness of this small-scale sequence is 11.65 m.

Medium-scale sequences

In both studied sections of the Opletnya Member, five medium-scale sequences have been identified, each subdivided into three parts — transgressive, maximum-flooding, and highstand deposits. The number of small-scale sequences within them, however, is not equal and varies from two to four (Fig. 7).

In all cases, the base of a medium-scale sequence is a prominent, laterally correlatable erosional surface. In the lowermost part, lithoclastic, bioclastic and/or ooid-dominated medium-scale transgressive deposits predominate. The small-scale sequences within this lower part are also developed mainly in transgressive facies, where limestones, often cross-bedded, predominate but dolomitic limestones are also present.

Intraclasts are also common and occupy the foreset laminae in cross-bedded structures but also form isolated lags. In almost all medium-scale sequences, the measured paleotransport indicators (planar and trough cross-bedding, reactivation and accretion surfaces) show a unidirectional pattern (towards the north-northeast; Fig. 7). Only in one case, at the base of the uppermost (fifth) medium-scale sequence, there are indications about short-term (and probably local) south-south-westward directions.

In the upper parts of the transgressive intervals of the medium-scale sequences, the amount of wacke- to mudstone beds and of beds with nodular structure and bioturbation increases. This trend reaches its maximum in the maximum-flooding zone. At the same time, an increase of the intensity and the scale of synsedimentary deformations is observed. Firm- and hard-ground development is also documented. From here upwards, medium-scale sequences commonly display an increasing diversification of the sedimentary paleotransport directions, and in many cases almost opposite directions can be observed in one and the same stratigraphic level.

In the highstand part of the medium-scale sequences, there commonly is an increase in the amount of dolomite and evaporites. Desiccation cracks and tepee structure are also common. The amount and the size of the intraclasts increases as well. Their roundness varies in a wide range, both vertically in a section and laterally. Occasionally, rudstone fills small-scale channels.

In the studied sections, the first medium-scale sequence is well defined and includes small-scale sequences 1 to 4, and elementary sequences 1 to 20. Small-scale sequences 5 and 6 compose a second medium-scale sequence. The thick high-energy deposits in small-scale sequences 7 and 8 then suggest the transgressive part of a third medium-scale sequence. Its top is difficult to place, but the relatively thin and complex elementary sequence 50 with an erosion surface at its base (Fig. 7d) may be interpreted as the limit to a fourth medium-scale sequence. This fourth sequence comprises small-scale sequences 11 and 12, and its top is defined by the prominent erosion surface An1. The top of the fifth medium-scale sequence cannot be defined in the studied sections and may be within the Lakatnik Member.

Cyclostratigraphic interpretation

The newly obtained biostratigraphical data (Ajdanlijsky et al. 2018; this study) allow estimating the time range of the sedimentary cycles documented in the studied sections. It mostly concerns the boundaries of the Aegean substage in the study area. Its base is defined in the uppermost part of the fluvial succession of the Petrohan Terrigenous Group, just below the base of the Svidol Formation by palynological data (Ajdanlijsky et al. 2018). The top of the substage is located in the uppermost part of the Opletnya Member of the Mogila Formation, as inferred from the last appearance of early Anisian palynomorphs (Fig. 3). The upper boundary of the Aegean is situated at the top of elementary sequence 60 of small-scale sequence 12 (Fig. 7d). The total number of elementary sequences recognized for the Aegean substage (Ajdanlijsky et al. 2018; this study) is 80 (1 in the uppermost Petrohan Terrigenous Group, 19 in the Svidol Formation, 60 in the Opletnya Member). Erosion certainly occurred at the boundaries of some elementary sequences as indicated by the irregular surfaces and the reworking (Fig. 7), but the regular stacking pattern does not suggest that entire sequences are missing.

Comparing this result to the new Triassic chart by Haq (2018) that proposes a duration of about 1.7 Myr for the Aegean, the average time duration of a single elementary sequence would be approximately 21.25 kyr. However, according to Ogg et al. (2016), the Aegean had a duration of 1.5 Myr, suggesting a duration of 18.75 kyr per elementary sequence. In the Middle Triassic, the periodicities of the orbital precession cycle had peaks at ca. 18 and 22 kyr (Berger et al. 1989), with an average of 20 kyr (Hinnov 2018). This is close to the estimated duration of the elementary sequences recorded in the Opletnya Member, which are consequently interpreted as being related to the precession cycle. The fact that 5 elementary cycles compose a small-scale sequence suggests that these were controlled by the short eccentricity cycle of 100 kyr (Hinnov 2018).

In the studied sections, the medium-scale sequences have been defined based on their lithology. The first one is well defined with 4 small-scale (100-kyr) and 20 elementary (20-kyr) sequences. Medium-scale sequences are in many cases induced by the long eccentricity cycle of 405 kyr (e.g., Strasser et al. 2000; Boulila et al. 2008). However, the interpretation of the other medium-scale sequences, comprising two or four small-scale sequences, is less clear: they may have resulted from a combination of allocyclic and autocyclic processes, obscuring a clear signal of the long eccentricity cycle.

The transgressive-regressive facies trends within the sequences of all scales imply that these were — at least partly — controlled by sea-level changes. Furthermore, the stacking of these sequences reflecting the hierarchy and durations of the orbital (Milankovitch) cycles suggests that the sea-level changes were in tune with the climate changes induced by the orbital cycles (e.g., Strasser 2018). However, the complexity of facies and sedimentary structures seen in the Opletnya Member also implies that additional factors such as lateral migration of sediment bodies were active.

Palynofacies

Concept

The term palynofacies was first introduced by Combaz in 1964 to describe the total acid-resistant organic matter content of sedimentary rocks within a specific depositional environment (Combaz 1964, 1980). Later, Tyson (1993, 1995) defined palynofacies analysis as a methodology involving the identification of individual palynomorphs, plant debris, and

amorphous components, their absolute and relative proportions, size spectra, and preservation states.

A number of sedimentary organic matter classifications and parameters are used in palynofacies analysis, reviewed in Tyson (1987, 1993, 1995). In this study, sedimentary organic matter is divided into a marine (autochthonous) fraction including marine phytoplankton and foraminiferal test linings, and a continental (allochthonous) fraction composed of pollen grains, spores, and phytoclasts (Rameil et al. 2000). The here used palynofacies parameters to decipher transgressive-regressive trends within the studied succession are: (1) the ratio of continental to marine constituents (CONT/MAR); (2) the ratio of opaque to translucent phytoclasts (OP/TR); (3) the phytoclast particle size and shape (equidimensional to blade-shaped; ED/BS); and (4) the relative proportion and species diversity of marine phytoplankton.

Palynofacies analysis

Within the studied Anisian succession, long-term transgressive–regressive trends are clearly documented in the CONT/MAR ratio and phytoplankton abundance with three distinct acritarch events (Fig. 3). A first marine pulse during the early Anisian (Aegean) was recognized by an acritarch peak in the lowermost Opletnya Member (basal part of the Mogila Formation) below the Tenuis Bed (Ajdanlijsky et al. 2018), characterized by a low-diversity marine invertebrate fauna (Tronkov 1968). A second acritarch peak occurs in the upper part of the Mogila Formation (base of the Lakatnik Member). The third acritarch peak in the Zimevitsa Member (lower part of the Babino Formation) is the most prominent signal accompanied by the highest diversity of marine invertebrates, including brachiopods and crinoids.

Short-term changes of sea level are documented in the changes of sedimentary organic matter content within sedimentary sequences: changes of terrestrial input, preservation and sorting of phytoclasts, and prominent phytoplankton peaks indicating major flooding phases. In the Lakatnik section (Fig. 14), a 4.5 m thick elementary sequence shows marine plankton percentages between 5.1 and 10.7 % in the basal grainstones (samples 1–3), the highest percentage occurring in the basal lithoclast bed. Translucent phytoclasts of different sizes and shapes are common. Upsection, a marked increase in phytoplankton is observed (samples 4, 5), with peak abundance (23.5 %) in sample 4, also characterized by the highest ratios of opaque to translucent (OP/TR) and equidimensional to blade-shaped (ED/BS) phytoclasts. High percentages of marine plankton and high OP/TR and ED/BS ratios continue in samples 6 and 7, while the uppermost part of the sequence (samples 8–9) shows low plankton percentages (3.6 to 6.5 %). Within the phytoplankton group, acritarchs are most abundant in samples 4 and 5, while prasinophytes are dominant in samples 8 and 9, and they are the only plankton group present in sample 10. Foraminiferal test linings are recorded in samples 3, 4, 5 and 7. Bisaccate pollen grains are the dominant group within the terrestrial particles, and spores are rare.

The basal grainstones (samples 1–3) are interpreted as transgressive deposits, showing a high amount of "fresh" translucent phytoclasts with a huge variety in sizes and shapes. A first plankton peak in the basal lithoclast bed marks the initial transgressive pulse. The sequence boundary might be directly overlain by the transgressive surface, which explains the lack of lowstand deposits. The level of sample 4 seems to indicate the maximum-flooding surface on top of the transgressive deposits with the most prominent plankton peak and the lowest ratio in continental to marine particles. Alternatively, the interval including sample 4 and 5 can be interpreted as maximum-flooding zone since plankton percentages are the highest, accompanied by the lowest ratio of continental to marine particles and the highest amount of equidimensional, opaque phytoclasts. The interval spanning samples 6 and 7 is interpreted as early highstand deposits where the percentages of marine plankton and equidimensional, opaque phytoclasts are still high and foraminiferal test linings are present but the influx of terrestrial particles is increasing. The change from an acritarch-dominated to a prasinophyte-dominated plankton assemblage recorded in the uppermost part of the succession (samples 8–10), as well as the switch to high terrestrial influx with blade-shaped and mixed opaque and translucent phytoclasts is interpreted as indicative of late highstand deposits. Prasinophytes are the only phytoplankton in sample 10, pointing to a restricted shallow depositional environment, most probably lagoonal. However, from the palynofacies data it remains an open question whether the dolomitic limestones captured by sample 10 represent the latest highstand deposits or lowstand deposits with the respective sequence boundary placed between sample 9 and 10, and the transgressive surface recorded by the lithoclasts at the base of the overlying grainstones.

The palynofacies analysis thus completes and refines the sequence- and cyclostratigraphic interpretation based on lithofacies and sedimentary structures.

Discussion

Biostratigraphy, chronostratigraphy, and large-scale correlations

The new biostratigraphic data obtained enable the discrimination of the Anisian substages and placement of their boundaries in the studied sections. The Aegean/Bithynian boundary is placed in the upper part of the Opletnya Member (lower Mogila Formation), and the Bithynian/Pelsonian boundary in the lower Zimevitsa Member (lower Babino Formation). Ajdanlijsky et al. (2018) have already identified the base of the Aegean substage (Olenekian/Anisian boundary) in the uppermost Petrohan Terrigenous Group (Fig. 3). Based on these data, a first precise timing of the sedimentary cyclicity within the lower Anisian succession in the area of the Iskar gorge becomes possible.

Large-scale cyclicity can be detected by phytoplankton abundances. A first marine pulse in the early Anisian

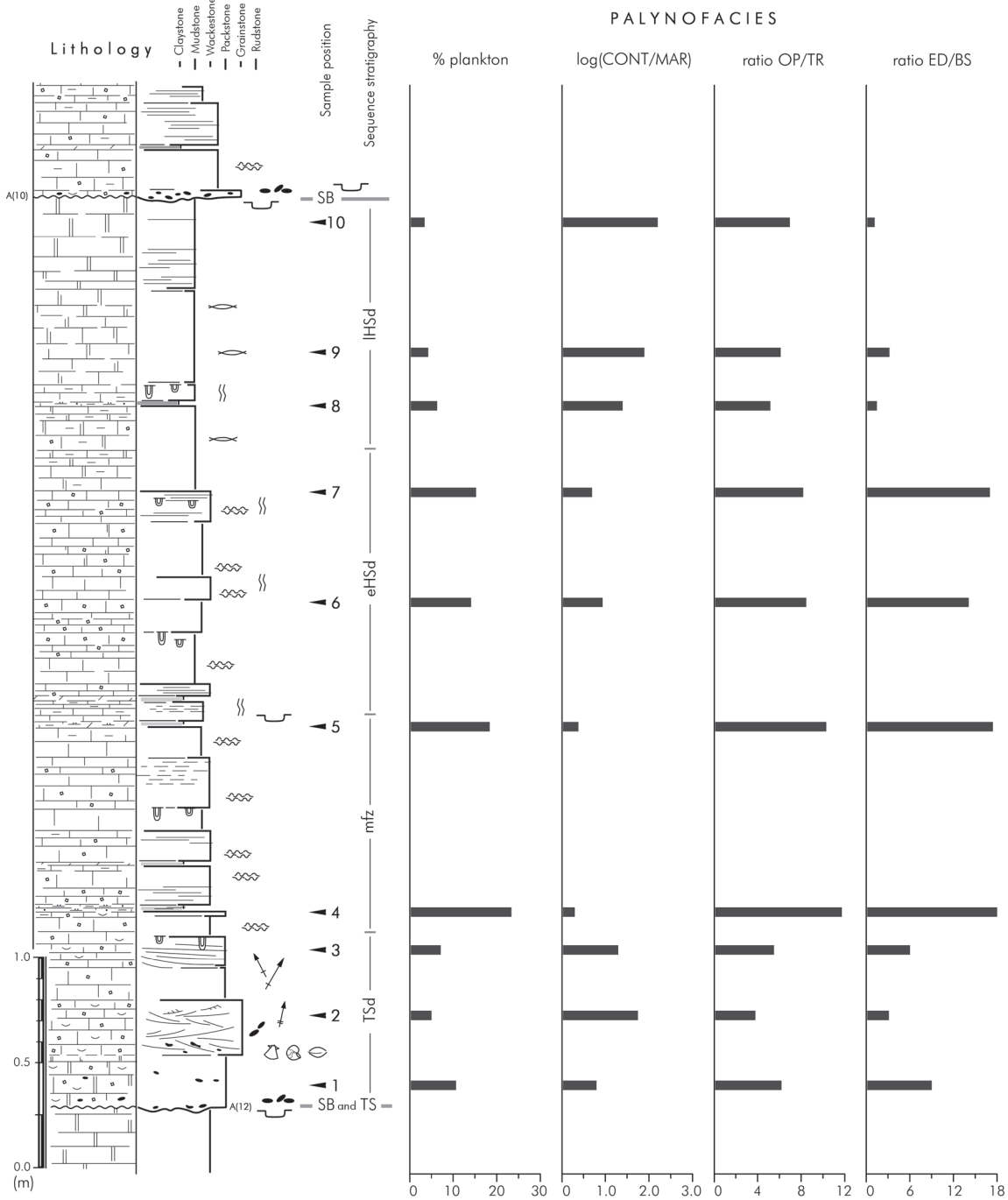

Fig. 14. Palynofacies patterns of elementary sequence 6 (lower Opletnya Member), exposed in a road cut 450 m west of the Lakatnik section. SB: sequence boundary; TS: transgressive surface; TSd: transgressive deposits; mfz: maximum-flooding zone; eHSd: early highstand deposits; lHSd: late highstand deposits. CONT: continental components; MAR: marine components; OP: opaque; TR: translucent; ED: equidimensional; BS: blade-shaped.

(lowermost Opletnya Member, 2 m below the Tenuis Bed) is followed by a prominent flooding event in the Bithynian (upper part of the Opletnya Member) and a third major flooding event in the Pelsonian (middle part of the Zimevitsa Member), documented by peak abundances of marine acritarchs. These three flooding phases were also detected in the Muschelkalk deposits of southern Poland (Matysik 2016). The most prominent transgressive signature in the Pelsonian is recorded in carbonate ramp systems along the western Tethys shelf (Michalík et al. 1992; Haas et al. 1995; Török 1998; Götz et al. 2003; Budai & Vörös 2006; Götz & Török 2008; Stefani et al. 2010; Chatalov 2013) and in characteristic transgressive facies successions in the northern Peri-Tethys basin (Szulc 2000; Feist-Burkhardt et al. 2008). It might reflect a global warming episode in the Pelsonian (Retallack 2013; Li et al. 2018).

Sedimentary cyclicity

Controversial interpretations of the prominent small-scale cyclicity in the lower part of the Iskar Carbonate Group are documented in publications of the last decades. Čatalov (1975) assumed that the Svidol Formation was formed under epicontinental tidal-flat conditions characterized by cyclic deposition. Later, Tronkov (1983, 1989) regarded the Opletnya Member of the Mogila Formation as a typical rhythmic succession and described the main features of these rhythms (hemicycles), subdividing them into three lithozones: (i) lower, formed by oolitic-bioclastic calcarenites with intraclasts; (ii) middle, characterized by marly limestones; and (iii) upper, made up of dolomites. The rhythms are defined by transgressive surfaces. According to the same author, the thickness of the individual sedimentary cycles in the lower Opletnya Member is in the range between 2 and 5 m, while upsection they can reach and even exceed 20 m. The same author assumed that these three lithozones represent (i) the distal offshore shelf bars, (ii) a calm back-bar carbonate sedimentation with limited water circulation, and (iii) isolated lagoon environments, respectively. The time duration and/or the rank of the cycles were not defined. He proposed that the most complete and detailed stratigraphic subdivision of the Opletnya Member could be achieved considering its rhythmic character, using each rhythm (hemicycle) as a distinct correlatable stratigraphic unit.

Chatalov (1998, 2000, 2004) described peritidal cycles in the lower Opletnya Member, discriminating a total of 17 small (meter)-scale shallowing-upward asymmetric cycles. The upper part of the member was not discussed. He assumed that each shallowing-upward cycle (hemicycle) formed in a tidal-flat environment due to sequential passage through its different bathymetric zone. As a result, from base to top, the ideal individual cycle is tripartite, starting with a subtidal basal lag, followed by subtidal mudstones and bioclastic wackestones, and ending with intertidal/supratidal dolomites. The thickness of these hemicycles varies from 1.1 m to 12.4 m, with an average of 4.4 m. According to Chatalov (2016, 2018), the influence of relative sea-level changes on the formation of these cycles is debatable and he proposed an autogenic control for the formation of these peritidal ramp cycles.

Ajdanlijsky et al. (2004) interpreted the entire succession of the Opletnya Member as a result of hierarchical cyclic processes. The smallest recognizable cyclic unit was defined as elementary cycle, beginning with a transgressive surface, often with an erosional base. The lower part of these cycles was deposited in a high-energy shallow-marine setting, during transgression over very shallow-marine (inter- or supratidal) deposits forming the uppermost part of the previous cycle. The top of the transgressive part of these cycles is marked by the deepest lithofacies, indicating maximum flooding. The upper part of the cycles demonstrates a shallowing-upwards trend. The elementary cycles are grouped into submesocycles, and these in turn into mesocycles with thicknesses of several tens of meters. Because of the absence of reliable biostratigraphic data, the time range of the elementary and submesocycles was not defined, but it was assumed that the mesocycles correspond to the third-order cycles of Vail et al. (1991).

Field data from both sections of the Opletnya Member obtained during the present study allow refining the previous interpretations by a precise definition and lateral correlation of regional bounding surfaces and individual cycles, as well as by an assessment of lateral lithofacies variations. The newly obtained biostratigraphic data enable to establish a time framework for the sequences of different hierarchical orders and to reinterpret the stacking pattern.

The smallest recognizable cyclic units are here called elementary sequences (following the concepts of Strasser et al. 1999). They are symmetrical with a deepening-upward trend in the lower and a shallowing-upward trend in the upper part, separated by a maximum-flooding surface. Their boundaries are represented by the shallowest lithofacies. In many cases, sequence boundary and transgressive surface are amalgamated, which is explained by the low accommodation on the shallow ramp. Lowstand deposits thus are only rarely preserved. Combined into packages of five, these elementary sequences form 14 larger cyclic units in the Opletnya Member, here defined as small-scale sequences.

The number of the smallest cyclic units distinguished in the underlying Svidol Formation, interpreted as parasequences, is 19 (Ajdanlijsky et al. 2018). Their thicknesses vary from 0.7 m to 2.9 m (average 1.45 m), similar to those of the elementary sequences in the Opletnya Member. These parasequences commonly combine into packages of five, with the maximum thickness recorded in the lower part of the transgressive interval of these packages. As scale and stacking pattern of the parasequences defined in the Svidol Formation and of the elementary sequences in the Zimevitsa Member are very similar to those of the elementary sequences in the Opletnya Member, a similar formation is assumed. The subsidence rate of the ramp must have been relatively constant throughout this time interval and allowed for enough accommodation to accumulate the observed sedimentary record. Although minor erosion and/or non-deposition certainly occurred at the boundaries of some elementary sequences, there is no evidence that entire sequences are missing (Strasser 2016).

Comparing the total number of the Aegean elementary and small-scale sequences with the updated Middle Triassic chart (Haq 2018), it can be concluded that they are documenting an allocyclic signal and formed in tune with the precession (20-kyr) and short eccentricity (100-kyr) orbital cycles, respectively. The 14 small-scale sequences identified in the Opletnya Member thus indicate that this member was deposited over a time period of 1.4 Myr. Furthermore, based on the similarities in the composition and thickness, it can be assumed that the elementary and small-scale sequences distinguished in the lowermost and uppermost Bithynian substage (i.e small-scale sequences 13 and 14 in the uppermost Opletnya Member and those from the lowermost Zimevitsa Member) also represent precession and short eccentricity cycles (Figs. 7, 10).

Concerning the medium-scale sequences, only the one recognized in the Svidol Formation by Ajdanlijsky et al. (2018) and the one at the base of the Opletnya Member (see above) can be attributed to the 405-kyr long eccentricity cycle. They are both composed of 4 small-scale sequences and 20 elementary sequences and thus reflect the hierarchical stacking characteristic of a sedimentary system controlled by orbital cycles (e.g., Strasser et al. 2006).

The highly variable lateral and vertical patterns of facies and sedimentary structures (see Chapter Sedimentology) clearly indicate that the shallow ramp hosted diverse sedimentary environments: from shallow marine to supratidal, from low to high energy, from normal marine to evaporative. These environments were subjected not only to sea-level fluctuations controlled by the orbital cycles but also to currents that shifted sediment bodies and to minor tectonic movements that had an additional control on accommodation. Consequently, the observed sedimentary record is the result of a combination of allocyclic as well as of autocyclic and random processes (e.g., Pratt & James 1986; Strasser 2018). From the cyclostratigraphic interpretation it appears that the amplitudes of the sea-level changes induced by the precessional and short eccentricity cycles were sufficient to create facies changes that were recorded on the shallow ramp, but that the amplitude related to the long eccentricity cycle left its traces only in the Svidol Formation and at the base of the Opletnya Member.

Major sequences

The interpretation of the small-scale sequences in the Opletnya Member as reflecting the short (100-kyr) eccentricity cycles allows the correlation with some of the major sequence boundaries of the Tethyan realm. Ajdanlijsky et al. (2018) correlated the base of the Svidol Formation with sequence boundary Ol4 in the upper Olenekian (Hardenbol et al. 1998; Ogg 2012). According to Li et al. (2018), the next major sequence boundary An1 is located 4 long (405-kyr) eccentricity cycles above the Ol4 boundary, which corresponds to 16 short (100-kyr) eccentricity cycles (Fig. 15). In the study area, the Svidol Formation contains four short eccentricity cycles that can be correlated with the long eccentricity cycle E13 of Li et al. (2018). Consequently, the position of sequence boundary An1 has to be placed at the boundary between the 12th and the 13th small-scale sequence (Fig. 7d), and this corresponds to the top of cycle E16 of Li et al. (2018). In the Opletnya Member, this boundary is marked by the relatively deepest local erosion of over 70 cm. The surface is covered by abundant lags of large intraclasts and marks the top of a 10 m thick dolomite-dominated interval with tepees, desiccation cracks, and abundant evaporites.

According to Haq (2018), sequence boundary Ol2 (equivalent to Ol4 of Hardenbol et al. 1998) just below the boundary between the Spathian and Aegean is dated at 246.9 Ma, and sequence boundary An1 in the upper Aegean at 245.5 Ma. This implies a duration of about 1.4 Myr for this major sequence. However, according to Li et al. (2018) and our own study (Fig. 15), the top of the Aegean coincides with sequence boundary An1 and the 16 small-scale sequences identified here between the two boundaries suggest a duration of 1.6 Myr (Fig. 15). This discrepancy calls for more research in radiometric dating and in astrochronology. For example, the date proposed for the Olenekian–Anisian (Spathian–Aegean) boundary has shifted from 247.1 Ma (Ogg 2012) to 246.8 (Ogg et al. 2016), to 246.9 Ma (Haq 2018), and then to 247.2 Ma in the IUGS International Chronostratigraphic Chart (2018, version 08).

The lithofacies data obtained in this study match well to the general facies trends in the major sequence bounded by Ol4 and An1. According to Li et al. (2018), its maximum-flooding surface is in the middle part of cycle E14 (Fig. 15). Based on the number of identified small-scale sequences above sequence boundary Ol4, this surface has to be placed in the maximum-flooding zone of the lowermost medium-scale sequence within the Opletnya Member, marked by muddy facies and a striking acritarch peak (Fig. 3). Upsection in the Opletnya Member, facies indicate decreasing water depth and the gradual establishment of peritidal environments, which led to precipitation of evaporites and early diagenetic dolomitization in the small-scale sequences at the top of this major sequence. The fact that the study of Li et al. (2018) is based on a deep-water section in South China implies that the general development of this sequence was controlled by over-regional parameters.

The identification of the next major sequence boundary (An2) is rather uncertain. On the one hand, the lithological and biostratigraphical data suggest that it could be situated at the top of the 5th elementary sequence of the Babino Formation (Fig. 10). This boundary marks an interruption in sedimentation with signs of subaerial exposure and development of a karstic surface that could have resulted from a prolonged time gap. On the other hand, its confident placement requires also reliable data for the cyclicity within the interval between boundaries An1 and An2. Such information is available for the uppermost Opletnya Member and lowermost Zimevitsa Member, while data on the cyclicity within the Lakatnik Member are not available yet. A peak abundance of marine acritarchs occurs in the Zimevitsa Member (Fig. 3) and probably corresponds to the maximum flooding identified by Li et al. (2018) below sequence boundary An2 (Fig. 15).

Soft-sediment deformation

Besides cyclicity, the sigmoidal structures resulting from soft-sediment deformation that occur in the lower part of the Opletnya Member can serve as a potential tool for event stratigraphy. Michalík (1997) interpreted these deformation structures as record of tsunamites and Chatalov (2001a,b, 2004) followed this interpretation of seismic activity during the Anisian. Eleven seismite horizons within muddy limestones were described from the Sfrazen and Lakatnik sections. In southern, western, and northern directions the number of

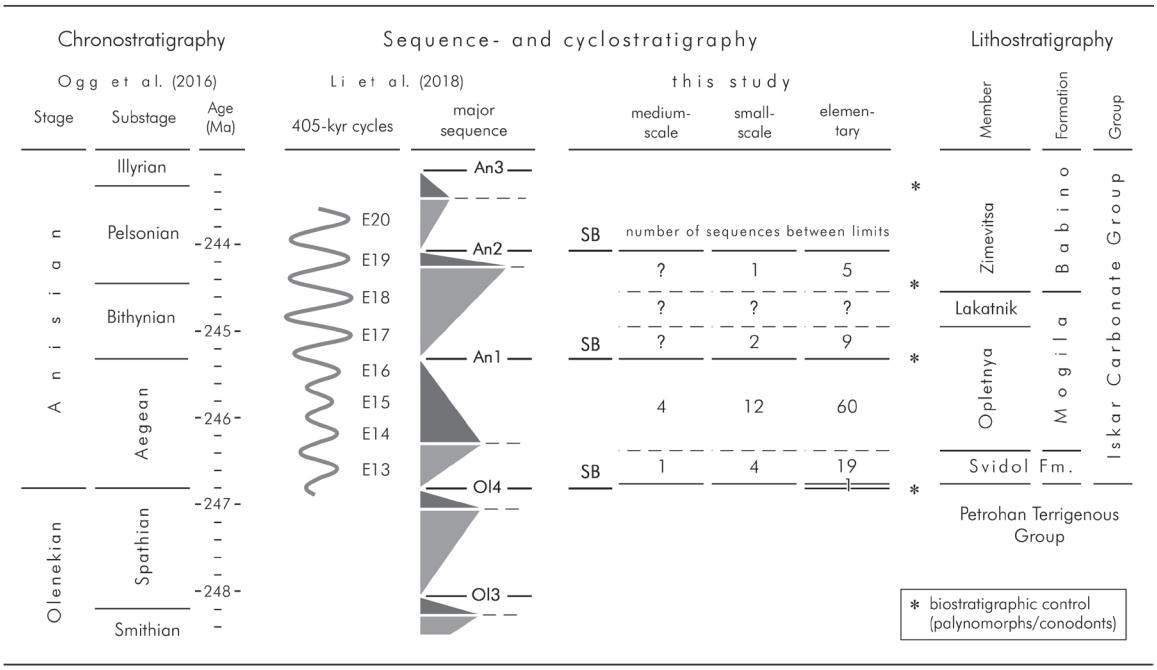

Fig. 15. Cyclostratigraphic chart of the Opletnya Member in the study area. See text for explanation.

these levels decreases, which might provide evidence of an ancient earthquake epicenter in the area of these two sections. However, no data showing their orientation were presented. Thus, the localization of a possible seismic epicenter remains unsettled.

In the studied sections, synsedimentary deformation is observed in mudstones, as well as in wacke- and wacke- to packstones (Fig. 6). The stratigraphic position of these deformation structures is specific: Ajdanlijsky et al. (2018) pointed out that they occur predominantly within the highstand stage of an elementary sequence. The newly obtained data confirm this observation and also shed new light on the facies context of these structures. Their position in the upper part of the elementary sequences, restricted lateral distribution, concave-up morphology on top of the individual beds, and their proximity and temporal correlation with small-scale cut-and-fill structures indicate that they most probably are connected with soft-sediment slumping activated by small-scale erosional events. Sliding on the steep flank of a channel could produce similar sedimentary structures. Furthermore, storm-induced loading of non-lithified, cohesive sediment may lead to thixotropic behavior (e.g., Chen & Lee 2013). Muddy sediment was more abundant during a highstand phase than during transgression, which might explain the preferential stratigraphic position of these features of soft-sediment deformation.

It has to be mentioned that the lateral distribution and scale of sigmoidal structures is much wider and larger than previously noted. For example, to the south of the study area, west of Tserovo village (Fig. 2), a laterally traceable horizon of such structures is almost half a meter thick and twice as high above the base of the Opletnya Member than the thickest level (40 cm) in the studied sections (Fig. 7). Again, this horizon is developed in the upper (highstand) part of an elementary sequence.

In our opinion, the sigmoidal deformation structures in the studied sections are paleoenvironmental indicators of the initiation of the shallowing trend within the sequences rather than seismites. However, a detailed lateral mapping of these structures, including orientation measurements within isochronous levels, is necessary to elucidate their origin.

Conclusions

The early Anisian (Aegean) ramp deposits of the Opletnya Member in northwestern Bulgaria feature a prominent cyclical pattern of the sedimentary record. In the two studied sections of Lakatnik and Sfrazen, the facies are carbonate-dominated but also include terrigenous siliciclastic material and evaporites, and are interpreted as having been deposited in a variety of environments ranging from peritidal to shallow marine. Deepening-shallowing trends of facies evolution and prominent surfaces allow identifying elementary, small-scale, and medium-scale sequences. Palynofacies analysis complements and confirms the lithofacies analysis within selected sequences. The sequences are hierarchically stacked, with 5 elementary sequences composing a small-scale one, and 2 or 4 small-scale sequences composing a medium-scale one. Biostratigraphic data (conodonts and palynomorphs) allow defining the Anisian substage boundaries, and thus provide the basis for an estimation of the durations of these sequences. Elementary and small-scale sequences are interpreted to reflect the signatures of the orbital precession and short eccentricity cycles with periodicities of 20 and 100 kyr, respectively. Accordingly, it is

suggested that the Opletnya Member, which comprises 69 elementary and 14 small-scale sequences (Fig. 15), was deposited within about 1.4 Myr. Medium-scale sequences that correspond to the long eccentricity cycle of 405 kyr have been identified only in the Svidol Formation and at the base of the Opletnya Member. This suggests that the translation of orbital cycles into sea-level changes that were then recorded on the shallow ramp was not straightforward, and that other processes inherent to the sedimentary system (such as lateral migration of sediment bodies) and/or changes in subsidence rate must have been at work as well.

Major sequence boundaries are identified at the base of the Svidol Formation and within the uppermost Opletnya Member, corresponding to the sequence boundaries Ol4 and An1 of the Tethyan realm. According to the cyclostratigraphic interpretation presented here, there are 16 small-scale sequences between these two sequence boundaries, implying a duration of 1.6 Myr. Large-scale flooding events are recognized by peak abundances of marine acritarchs, with the most prominent event being identified in the Pelsonian Zimevitsa Member. This Pelsonian maximum flooding is recorded in carbonate ramp systems along the western Tethys shelf and in the northern Peri-Tethys basin.

This study demonstrates that, based on detailed logging and facies analysis, a cyclostratigraphic interpretation of shallow ramp deposits is possible. Within a time framework based on biostratigraphy and chronostratigraphy, the duration of individual meter-scale depositional sequences can be estimated, and a time resolution of 20 kyr can be achieved to better interpret the evolution of the sedimentary environments. Furthermore, astrochronologically dated correlation with regional and over-regional events becomes possible and places the studied Bulgarian sections in a global context.

Acknowledgements: This study is part of the Triassic Ocean project TRIO lead by A.E. Götz. The thorough review of Janos Haas (Budapest) and the comments of the handling editor Jozef Michalík (Bratislava) are gratefully acknowledged.

References

Adams A., Diamond L.W. & Aschwanden L. 2018: Dolomitization by hypersaline reflux into dense groundwaters as revealed by vertical trends in strontium and oxygen isotopes: upper Muschelkalk, Switzerland. *Sedimentology* 66, 362–390.

Ajdanlijsky G., Tronkov D. & Strasser A. 2004: Cyclicity in the Lower Triassic Series between Opletnya railway station and Sfrazen hamlet. In: Sinnyovsky D. (Ed.): Geological routes in the northern part of the Iskar River Gorge. *V. Nedkov Publ.*, 90–101.

Ajdanlijsky G., Götz A.E. & Strasser A. 2018: The Early to Middle Triassic continental–marine transition of NW Bulgaria: Sedimentology, palynology and sequence stratigraphy. *Geol. Carpath.* 69, 2, 129–148.

Assereto R. & Čatalov G. 1983: The Mogila Formation (Lower–Middle Triassic) and lithostratigraphical levels in the Triassic System of NW Bulgaria. *Geologica Balc.* 13, 6, 29–36 (in Russian).

Assereto R., Tronkov D. & Čatalov G. 1983: The Mogila Formation (Lower–Middle Triassic) in Western Bulgaria. *Geologica Balc.* 13, 6, 25–27 (in Bulgarian).

Benatov S. 1998: An attempt for biostratigraphic zonation of West Bulgarian Middle Triassic on benthonic macrofauna. *C.R. Bulg. Acad. Sci.* 51, 11–12, 69–72.

Benatov S. 2000: Macrofauna from Peri-Tethyan Middle Triassic in the southern slopes of Western Stara Planina Mountain (Western Bulgaria). In: Bachmann G.H. & Lerche I. (Eds.): Epicontinental Triassic, Volume 2. *Zbl. Geol. Paläont.*, *Teil I (1998)*, 9/10, 1137–1144.

Benatov S. 2001: Brachiopod biostratigraphy of the Middle Triassic in Bulgaria and comparison with elsewhere in Europe. In: Brunton H., Robin L., Cocks M. & Long, S.M. (Eds.): Brachiopods Past and Present. *The Systematics Association Special Volume Series* 63, 384–393.

Benatov S. & Chatalov A. 2000: New data about the stratigraphy and lithology of the Iskar Carbonate Group (Lower–Middle Triassic) in the Zaburde district, Western Bulgaria. *Ann. Univ. Sofia "St. Kliment Ohridski", Fac. Geol. Geogr.* 93, vol. 1 — geology, 83–105.

Benatov S., Budurov K., Trifonova E. & Petrunova L. 1999: Parallel biostratigraphy on micro- and megafauna and new data about the age of the Babino Formation (Middle Triassic) in the Iskur Gorge, Western Stara Planina Mountains. *Geologica Balc*. 29, 33–40.

Benton M.J. 2015: When Life Nearly Died: The Greatest Mass Extinction of All Time. *Thames & Hudson*, London, 1–352.

Berger A., Loutre M.F. & Dehant V. 1989: Astronomical frequencies for pre-Quaternary palaeoclimate studies. *Terra Nova* 1, 474–479.

Borkhataria R., Aigner T. & Pipping K.J.C.P. 2006: An unusual, muddy, epeiric carbonate reservoir: The Lower Muschelkalk (Middle Triassic) of the Netherlands. *AAPG Bull.* 90, 1, 61–89.

Boulila S., Galbrun B., Hinnov L.A. & Collin P.-Y. 2008: High-resolution cyclostratigraphic analysis from magnetic susceptibility in a Lower Kimmeridgian (Upper Jurassic) marl-limestone succession (La Méouge, Vocontian Basin, France). *Sediment. Geol.* 203, 54–63.

Budai T. & Vörös A. 2006: Middle Triassic platform and basin evolution of the Southern Bakony Mountains (Transdanubian Range, Hungary). *Riv. Ital. Paleont. S.* 112, 359–371.

Budurov K. 1976: Die triassischen Conodonten des Ostbalkans. *Geologica Balc.* 6, 2, 95–104.

Budurov K. 1980: Conodont Stratigraphy of the Balkanide Triassic. *Riv. Ital. Paleont.* 85, 3–4, 767–780.

Budurov K. & Petrunova L. 2000: Muschelkalk conodonts as components of Peri-Tethyan fauna. In: Bachmann G.H. & Lerche I. (Eds.): Epicontinental Triassic, Volume 2. *Zbl. Geol. Paläont.*, *Teil I (1998)*, 9/10, 989–995.

Budurov K. & Stefanov S.A. 1972: Plattform-Conodonten und ihre Zonen in der Mittleren Trias Bulgariens. *Mitt. Ges. Geol. Bergbaustud*. 21, 829–852.

Budurov K. & Stefanov S.A. 1973: Etliche neue Platform-Conodonten aus der Mitteltrias Bulgariens. *C. R. Acad. Bulg. Sci.* 26, 803–806.

Budurov K. & Stefanov S.A. 1975: Neue Daten über die Conodontenchronologie der balkaniden Mittleren Trias. *C. R. Acad. Bulg. Sci.* 28, 791–794.

Budurov K. & Trifonova E. 1984: Correlation of Triassic conodont and foraminiferal zonal standards in Bulgaria. *C. R. Acad. Bulg. Sci.* 37, 625–627.

Budurov K. & Trifonova E. 1995: Conodont and foraminiferal successions from the Triassic of Bulgaria. *Geologica Balc.* 25, 13–19.

Budurov K., Trifonova E. & Zagorčev I. 1995: The Triassic in southwest Bulgaria. Stratigraphic correlation of key sections in the Iskar Carbonate Group. *Geologica Balc.* 25, 27–59.

Budurov K., Zagorchev I., Trifonova E. & Petrunova L. 1997: The Triassic in Eastern Stara planina Mts. Lithostratigraphic notes. *Rev. Bulg. Geol. Soc.* 58, 2, 101–110.

Čatalov G. 1975: Facies analysis of the Svidol Formation (Lower Triassic) of the Teteven anticlinorium (Central Fore-Balkan). *Geologica Balc.* 5, 2, 67–86.

Čatalov G. & Visscher H. 1990: Palynomorphs from Stoilovo Formation, Veleka Group (Triassic), Strandža Mountain, Southeast Bulgaria. *Geologica Balc*. 20, 2, 53–57.

Catuneanu O. 2019: Scale in sequence stratigraphy. *Mar. Petrol. Geol.* 106, 128–159.

Catuneanu O., Abreu V., Bhattacharya J.P., Blum M.D., Dalrymple R.W., Eriksson P.G., Fielding C.R., Fisher W.L., Galloway W.E., Gibling M.R., Giles K.A., Holbrook J.M., Jordan R., Kendall C.G.St.C., Macurda B., Martinsen O.J., Miall A.D., Neal J.E., Nummedal D., Pomar L., Posamentier H.W., Pratt B.R., Sarg J.F., Shanley K.W., Steel R.J., Strasser A., Tucker M.E. & Winker C. 2009: Towards the standardization of sequence stratigraphy. *Earth-Sci. Rev.* 92, 1–33.

Chatalov G. 1980: Two facies types of Triassic in Strandza Mountain, Bulgaria. *Riv. Ital. Paleont. S.* 85, 3/4, 1029–1046.

Chatalov G. 1991: Triassic in Bulgaria — a review. *Bull. Tech. Univ. Istanbul* 44, 1/2, 103–135.

Chatalov A. 1997: Sedimentology of the carbonate rocks from the Mogila Formation in Western Balkanides. *PhD Thesis Abstract, Sofia University "St. Kl. Ohridski"*, 1–46 (in Bulgarian).

Chatalov A. 1998: Arid carbonate tidal flat sedimentation imprinted in the Mogila Formation (Spathian-Anisian) from the Western Balkanides, Bulgaria. *Hallesches Jahrb. Geowiss. Reihe B*, Beih. 5, 32–33.

Chatalov A. 2000: The Mogila Formation (Spathian-Anisian) in the Western Balkanides of Bulgaria — ancient counterpart of an arid peritidal complex. In: Bachmann G.H. & Lerche I. (Eds.): Epicontinental Triassic, Volume 2. *Zbl. Geol. Paläont.*, *Teil I (1998)*, 9/10, 1123–1135.

Chatalov A. 2001a: Deformational structures in the Iskar Carbonate group (Lower-Upper Triassic) from the Western Balkanides. *Geologica Balc*. 30, 3–4, 43–57.

Chatalov A. 2001b: Signature of paleoseismic activity in the Triassic carbonate rocks from Northwestern Bulgaria. *Sediment 2001*, Jena, Abstract Vol., 29.

Chatalov A. 2004: Route VIII. Sedimentological sites in the carbonate Triassic between Lakatnik railway station and Opletnya village. In: Sinnyovsky D. (Ed.): Geological routes in the northern part of the Iskar River Gorge. *V. Nedkov Publ.*, 102–116.

Chatalov A. 2013: A Triassic homoclinal ramp from the Western Tethyan realm, Western Balkanides, Bulgaria: Integrated insight with special emphasis on the Anisian outer to inner ramp facies transition. *Palaeogeogr. Palaeoclimatol. Palaeoecol.* 386, 34–58.

Chatalov A. 2016: Dominant autogenic control on the formation of peritidal cycles in the Olenekian carbonate succession of NW Bulgaria. *Geosciences 2016*, Abstract Vol., 109–110.

Chatalov A. 2018: Global, regional and local controls on the development of a Triassic carbonate ramp system, Western Balkanides, Bulgaria. *Geol. Mag.* 155, 641–673.

Chatalov A., Benatov S. & Vangelov D. 2001: New data about the holostratotype of the Babino Formation (Middle Triassic). *Ann. Univ. Sofia "St. Kliment Ohridski", Fac. Geol. Geogr.* 94, Vol. 1 – geology, 27–40.

Chemberski G., Vaptsarova A. & Monahov I. 1974: Lithostratigraphy of the Triassic variegated terrigenous-carbonate and carbonate sediments studied with deep drilling in Northwestern and Central North Bulgaria. *Ann. DSO Geol. Res.* 20, 327–341 (in Bulgarian).

Chen J. & Lee H.S. 2013: Soft-sediment deformation structures in Cambrian siliciclastic and carbonate storm deposits (Shandong Province, China): Differential liquefaction and fluidization triggered by storm-wave loading. *Sediment. Geol.* 288, 81–94.

Chen Y.L., Krystyn L., Orchard M.J., Lai X.L. & Richoz S. 2015: A review of the evolution, biostratigraphy, provincialism, and diversity of Middle and early Late Triassic conodonts. *Pap. Palaeontol.* 2, 235–263.

Chen Y., Scholze F., Richoz S. & Zhang Z. 2019: Middle Triassic conodont assemblages from the Germanic Basin: implications for multi-element taxonomy and biogeography. *J. Syst. Palaeontol.* 17, 5, 359–377.

Chrząstek A. 2013: Trace fossils from the Lower Muschelkalk of Raciborowice Górne (North Sudetic Synclinorium, SW Poland) and their palaeoenvironmental interpretation. *Acta Geol. Polon*. 63, 3, 315–353.

Combaz A. 1964: Les palynofaciès. *Rev. Micropaléont.* 7, 205–218.

Combaz A. 1980: Les kérogènes vus au microscope. In: Durand B. (Ed.): Kerogen: Insoluble organic matter from sedimentary rocks. *Edition Technip*, 55–111.

Escudero-Mozo M.J., Márquez-Aliaga A., Goy A., Martín-Chivelet J., López-Gómez J., Márquez L., Arche A., Plasencia P., Pla C., Marzo M. & Sánchez-Fernández D. 2015: Middle Triassic carbonate platforms in eastern Iberia: Evolution of their fauna and palaeogeographic significance in the western Tethys. *Palaeogeogr. Palaeoclimatol. Palaeoecol.* 417, 236–260.

Feist-Burkhardt S., Götz A.E., Szulc J. (coordinators), Borkhataria R., Geluk M., Haas J., Hornung J., Jordan P., Kempf O., Michalík J., Nawrocki J., Reinhardt L., Ricken W., Röhling H.-G., Rüffer T., Török Á. & Zühlke R. 2008: Triassic. In: McCann T. (Ed.): The Geology of Central Europe. Vol. 2. *Geological Society,* London, 749–821.

Flügel E. 2004: Microfacies of Carbonate Rocks. *Springer*, Berlin, 1–976.

Ganev M. 1974: Stand der Kenntnisse über die Stratigraphie der Trias Bulgariens. In: Zapfe H. (Ed.): Die Stratigraphie der alpin-mediterranen Trias. Symposium Wien, *Schriftenr. Erdwissenschaftl. Komm., Österr. Akad. d. Wissenschaften*, Bd. 2, 93–96.

Głuchowski E. & Salamon M. 2005: The Lower Muschelkalk crinoids from Raciborowice, North-Sudetic Basin, SW Poland. *Geol. Quarterly* 49, 1, 83–92.

Gonzalez R. & Eberli G.P. 1997 : Sediment transport and bedforms in a carbonate tidal inlet; Lee Stocking Island, Exumas, Bahamas. *Sedimentology* 44, 1015–1030.

Götz A.E. 1996: Fazies und Sequenzanalyse der Oolithbänke (Unterer Muschelkalk, Trias) Mitteldeutschlands und angrenzender Gebiete. *Geol. Jb. Hessen* 124, 67–86.

Götz A.E. & Török Á. 2008: Correlation of Tethyan and Peri-Tethyan long-term and high-frequency eustatic signals (Anisian, Middle Triassic). *Geol. Carpath.* 59, 4, 307–317.

Götz A.E. & Török Á. 2018: Muschelkalk ramp cycles revisited. In: Montenari M. (Ed.): Stratigraphy & Timescales, vol. 3: Cyclostratigraphy and Astrochronology, 265–284.

Götz A.E., Török Á., Feist-Burkhardt S. & Konrád Gy. 2003: Palynofacies patterns of Middle Triassic ramp deposits (Mecsek Mts., S Hungary): A powerful tool for high-resolution sequence stratigraphy. *Mitt. Ges. Geol. Bergbaustud. Österr.* 46, 77–90.

Götz A.E., Luppold F.W. & Hagdorn H. 2019: Biostratigraphie und Zonierung der Conodonten des Muschelkalks. In: Deutsche Stratigraphische Kommission (Ed.): Stratigraphie von Deutschland XIII. Muschelkalk. *Schriftenr. Dt. Ges. Geowiss.* 91, in press.

Haas J., Kovács S. & Török Á. 1995: Early Alpine shelf evolution in the Hungarian segment of the Tethys margin. *Acta Geol. Hung*. 38, 95–110.

Haas J., Budai T. & Raucsik B. 2012: Climatic controls on sedimentary environments in the Triassic of the Transdanubian Range (Western Hungary). *Palaeogeogr. Palaeoclimatol. Palaeoecol*. 353–355, 31–44.

Hagdorn H. & Głuchowski E. 1993: Palaeobiogeography and stratigraphy of Muschelkalk echinoderms (Crinoidea, Echinoidea) in Upper Silesia. In: Hagdorn H. & Seilacher A. (Eds.): Muschelkalk. Schöntaler Symposium 1991. *Goldschneck*, Korb, 165–176.

Hardenbol J., Thierry J., Farley M., Jacquin T., de Graciansky P.-C. & Vail P. 1998: Mesozoic and Cenozoic sequence chronostratigraphic framework of European basins. *SEPM Spec. Publ.* 60, 1–13.

Hardie L.A. & Garrett P. 1977: General environmental setting. In: Hardie L.A. (Ed.): Sedimentation on the Modern Carbonate Tidal Flats of Northwest Andros Island, Bahamas. *John Hopkins University, Stud. Geol.* 22, 12–49.

Hardie L.A. & Ginsburg R.N. 1977: Layering: the origin and environmental significance of lamination and thin bedding. In: Hardie L.A. (Ed.): Sedimentation on the Modern Carbonate Tidal Flats of Northwest Andros Island, Bahamas. *John Hopkins University, Stud. Geol.* 22, 50–123.

Haq B.U. 2018: Triassic eustatic variations re-examined. *GSA Today* 28, https://doi.org/10.1130/GSATG381A.1.

Heunisch C. 1999: Die Bedeutung der Palynologie für Biostratigraphie und Fazies in der Germanischen Trias. In: Hauschke N. & Wilde V. (Eds.): Trias — eine ganz andere Welt, Europa am Beginn des Erdmittelalters. *Pfeil-Verlag*, München, 207–220.

Heunisch C. 2019: Palynomorphs of the Muschelkalk. In: Deutsche Stratigraphische Kommission (Ed.): Stratigraphie von Deutschland XIII. Muschelkalk. *Schriftenr. Dt. Ges. Geowiss.* 91, in press.

Hillgärtner H., Dupraz C. & Hug W. 2002: Microbially induced cementation of carbonate sands: are micritic meniscus cements good indicators of vadose diagenesis? *Sedimentology* 48, 117–131.

Hinnov L.A. 2013: Cyclostratigraphy and its revolutionizing applications in the Earth and planetary sciences. *GSA Bull.* 125, 1703–1734.

Hinnov L.A. 2018: Cyclostratigraphy and astrochronology in 2018. In: Montenari M. (Ed.): Stratigraphy & Timescales, vol. 3: Cyclostratigraphy and Astrochronology. *Acad. Press*, 1–80.

Ivanov Zh. 1998: Tectonics of Bulgaria. *Unpubl. Habil. Thesis. Sofia University "St. Kliment Ohridski"*, 1–634 (in Bulgarian).

IUGS International Chronostratigraphic Chart 2018: International Commission on Stratigraphy, version 2018/08. www.stratigraphy.org.

Kalvacheva R.K. & Čatalov G.A. 1974: Palynomorphen aus phyllitoiden Tonschiefern des Strandza-Gebirges. *C. R. Acad. Bulg. Sci.* 27, 10, 1419–1422.

Knaust D. 1998: Trace fossils and ichnofabrics on the Lower Muschelkalk carbonate ramp (Triassic) of Germany: tool for high-resolution sequence stratigraphy. *Geol. Rundsch*. 87, 21–31.

Knaust D. 2007: Invertebrate trace fossils and ichnodiversity in shallow-marine carbonates of the German Middle Triassic (Muschelkalk). In: Bromley R.G., Buatois L., Mángano G., Genise J.F. & Melchor R.N. (Eds.): Sediment–Organism Interactions: A Multifaceted Ichnology. *SEPM Spec. Publ.* 88, 221–238.

Knaust D., Curran H.A. & Dronov A.V. 2012: Shallow-marine carbonates. In: Knaust D. & Bromley R.G. (Eds.): Trace fossils as indicators of sedimentary environments. *Dev. Sedimentol.* 64, 705–750.

Kustatscher E. & Roghi G. 2006: Anisian palynomorphs from the Dont Formation of the Kühwiesenkopf/Monte Prà Della Vacca Section (Northern Italy). *Micropalaeontology* 52, 3, 223–244.

Li M., Huang C., Hinnov L., Chen W., Ogg J. & Tian W. 2018: Astrochronology of the Anisian stage (Middle Triassic) at the Guandao reference section, South China. *Earth Planet. Sci. Lett.* 482, 591–606.

Lukoczki G., Haas J., Gregg J.M., Machel H.G., Kele S. & John C.M. 2019: Multi-phase dolomitization and recrystallization of Middle Triassic shallow marine-peritidal carbonates from the Mecsek Mts. (SW Hungary), as inferred from petrography, carbon, oxygen, strontium and clumped isotope data. *Mar. Petrol. Geol.* 101, 440–458.

Matysik M. 2016: Facies types and depositional environments of a morphologically diverse carbonate platform: a case study from the Muschelkalk (Middle Triassic) of Upper Silesia, Southern Poland. *Ann. Soc. Geol. Polon*. 86, 119–164.

Michalík J. 1997: Tsunamites in a storm-dominated Anisian carbonate ramp (Vysoká Formation, Malé Karpaty Mts., Western Carpathians). *Geol. Carpath.* 48, 4, 221–229.

Michalík J., Masaryk P., Lintnerová O., Papšová J., Jendrejáková O. & Reháková D. 1992: Sedimentology and facies of a storm-dominated Middle Triassic carbonate ramp (Vysoká Formation, Malé Karpaty Mts., Western Carpathians). *Geol. Carpath.* 43, 4, 213–230.

Montañez I.A. & Osleger D.A. 1993: Parasequence stacking patterns, third-order accommodation events, and sequence stratigraphy of Middle to Upper Cambrian platform carbonates, Bonanza King Formation, southern Great Basin. *AAPG Mem.* 57, 305–326.

Montenat C., Barrier P., Ott d'Estevou P. & Hibsch C. 2007: Seismites: An attempt at critical analysis and classification. *Sediment. Geol*. 196, 5–30.

Niedźwiedzki R. & Salamon M., 2006: Triassic crinoids from the Tatra Mountains and their stratigraphic significance (Poland). *Geol. Carpath.* 57, 2, 69–77.

Ogg J. 2012: Triassic. In: Gradstein F., Ogg J., Schmitz M. & Ogg G. (Eds.): The geological time scale 2012. *Elsevier*, Amsterdam, 681–730.

Ogg J.G., Ogg G.M. & Gradstein F.M. 2016: The Concise Geologic Time Scale 2016. *Elsevier*, Amsterdam, 1–234.

Petrash D.A., Bialik O.M., Bontognali T.R.R., Vasconcelos C., Roberts J.A., McKenzie J.A. & Konhauser K.O. 2017: Microbially catalyzed dolomite formation: From near-surface to burial. *Earth Sci. Rev.* 171, 558–582.

Petrunova L. 1992a: First palynological evidence of the Ladinian Age of the Preslav Formation in Northwest Bulgaria. *Geol. Bulgarica* 22, 2, 46.

Petrunova L. 1992b: Palynological evidence of the Early Karnian Age of the Moesian Group in Northwest Bulgaria. *Geol. Bulgarica* 22, 2, 94.

Petrunova L. 1999: Palynological correlations of the Preslav Formation (Iskur Carbonate Group) to the Peri-Tethyan Triassic of Central Europe. *Geol. Bulgarica* 29, 1–2, 136.

Petrunova L. 2000: Palynomorphs around the boundary Lower–Middle Triassic from an olistolith in Eastern Stara Planina Mountains, Bulgaria. In: Proceed. Int. Workshop on the Lower–Middle Triassic (Olenekian-Anisian) boundary. Tulcea, Romania, 53–55.

Philip J., Masse J. & Camoin G. 1996: Tethyan carbonate platforms. In: Nairn A.E.M., Ricou L.-E., Vrielynck B. & Dercourt J. (Eds.): The Ocean Basins and Margins. Vol. 8. The Tethys Ocean. *Plenum Press*, New York–London, 239–266.

Pöppelreiter M. 2002: Facies, cyclicity and reservoir properties of the Lower Muschelkalk (Middle Triassic) in the NE Netherlands. *Facies* 46, 119–132.

Posamentier H.W., Allen G.P. & James D.P. 1992: High-resolution sequence stratigraphy — the East Coulee delta, Alberta. *J. Sediment. Petrol.* 62, 310–317.

Pratt B.R. & James N.P. 1986: The St George Group (Lower Ordovician) of western Newfoundland: tidal flat island model for carbonate sedimentation in shallow epeiric seas. *Sedimentology* 33, 313–343.

Rameil N., Götz A.E. & Feist-Burkhardt S. 2000: High-resolution sequence interpretation of epeiric shelf carbonates by means of palynofacies analysis: an example from the Germanic Triassic (Lower Muschelkalk, Anisian) of East Thuringia, Germany. *Facies* 43, 123–144.

Reineck H.-E. & Singh I.B. 1975: Depositional Sedimentary Environments. *Springer*, Berlin, 1–439.

Retallack G.J. 2013: Permian and Triassic greenhouse crises. *Gondwana Res*. 24, 90–103.

Rychliński T. & Szulc J. 2005: Facies and sedimentary environments of the Upper Scythian–Carnian succession from the Belanské Tatry Mts., Slovakia. *Ann. Soc. Geol. Polon*. 75, 155–69.

Stampfli G.M., Hochard C., Vérard C., Wilhem C. & von Raumer J. 2013: The formation of Pangea. *Tectonophysics* 593, 1–19.

Stefani M., Furin S. & Gianolla P. 2010: The changing climate framework and depositional dynamics of the Triassic carbonate platforms from the Dolomites. *Palaeogeogr. Palaeoclimatol. Palaeoecol.* 290, 43–57.

Strasser A. 2016: Hiatuses and condensation: an estimation of time lost on a shallow carbonate platform. *Depositional Record* 1, 91–117.

Strasser A. 2018: Cyclostratigraphy of shallow-marine carbonates — limitations and opportunities. In: Montenari M. (Ed.): Stratigraphy & Timescales, vol. 3: Cyclostratigraphy and Astrochronology, 151–187.

Strasser A., Pittet B., Hillgärtner H. & Pasquier J.-B. 1999: Depositional sequences in shallow carbonate-dominated sedimentary systems: concepts for a high-resolution analysis. *Sediment. Geol.* 128, 201–221.

Strasser A., Hillgärtner H., Hug W. & Pittet B. 2000: Third-order depositional cycles reflecting Milankovitch cyclicity. *Terra Nova* 12, 303–311.

Strasser A., Hilgen F.J. & Heckel P.H. 2006: Cyclostratigraphy — concepts, definitions and applications. *Newsl. Stratigraphy* 42, 75–114.

Szulc J. 2000: Middle Triassic evolution of the northern Peri-Tethys area as influenced by early opening of the Tethys ocean. *Ann. Soc. Geol. Polon*. 70, 1–48.

Török Á. 1998: Controls on development of Mid-Triassic ramps: examples from southern Hungary. In: Wright, V.P. & Burchette T.P. (Eds.): Carbonate ramps. *Geol. Soc. London, Spec. Publ.* 149, 339–367.

Toula F. 1878: Geologische Untersuchungen im westlichen Theile des Balkan und in angrenzenden Gebieten. VII Ein geologisches Profil von Vraca an der Isker und durch die Iskerschluchten nach Sofia. *Sitzber. d. k. Akad. Wissenschaften Wien* 77, 247–317.

Tronkov D. 1960: About the Triassic stratigraphy in Iskar River Gorge. *Ann. Geol. res. Direct.* 10, 131–153.

Tronkov D. 1968: The Lower–Middle Triassic boundary in Bulgaria. *Comm. geol. inst. Bulg. Acad. Sci., paleont. ser.* 17, 113–130 (in Bulgarian).

Tronkov D. 1973: Grundlagen der Stratigraphie der Trias im Belogradčik Antiklinorium (Nordwest Bulgarien). *Bull. Geol. Inst., ser. Strat. Lithol.* 22, 73–98.

Tronkov D. 1976: Triassische Ammoniten-Sukzessionen im Westlichen Balkangebirge in Bulgarien. *C. R. Acad. bulg. sci.* 29, 9, 1325–1328.

Tronkov D. 1981: Stratigraphy of the Triassic System in part of the Western Srednogorie (West Bulgaria). *Geologica Balc.* 11, 1, 3–20 (in Russian).

Tronkov D. 1983: The Mogila Formation (Lower–Middle Triassic) in Iskar River Gorge and Vratza Mountain (Western Stara Planina Mountain). *Geologica Balc.* 13, 6, 37–52 (in Russian).

Tronkov D. 1989: The carbonate Triassic in Lakatnik section. In: Nachev I. (Ed.): Stratigraphy and sedimentology of the Phanerozoic in Bulgaria. XIV Congr. Carp.-Balk. Geol. Assoc., Field guide, 27–29 (in Russian).

Tronkov D. 1992: Godec Formation and Mazgoska Formation — two new Middle Triassic lithostratigraphic units in the Western Stara Planina mountain. *Geologica Balc.* 22, 6, 62.

Tronkov D. 1995: *Triassic System*. In: Haydutov I. (Ed.): Explanation notes to the geological map of Bulgaria on scale 1:100,000, Berkovitca map sheet. *Avers*, Sofia, 44–59 (in Bulgarian).

Tronkov D., Encheva M. & Trifonova T. 1965: Stratigraphy of the Triassic system in north-western Bulgaria. *Proc. Geol. Inst., Bulgarian Academy of Sciences* 14, 261–292.

Tyson R.V. 1987: The genesis and palynofacies characteristics of marine petroleum source rocks. In: Brooks J. & Fleet A.J. (Eds.): Marine Petroleum Source Rocks. *Geol. Soc. Spec. Publ.* 26, 47–67.

Tyson R.V. 1993: Palynofacies analysis. In: Jenkins D.G. (Ed.): Applied Micropaleontology. *Kluwer Academic Publishers*, Dordrecht, 153–191.

Tyson R.V. 1995: Sedimentary organic matter: organic facies and palynofacies. *Chapman & Hall*, London, 1–615.

Vail P.R., Audemard F., Bowman S.A., Eisner P.N. & Perez-Cruz C. 1991: The stratigraphic signatures of tectonics, eustasy and sedimentology — an overview. In: Einsele G., Ricken W. & Seilacher A. (Eds.): Cycles and Events in Stratigraphy. *Springer*, Berlin, 617–659.

van Wagoner J., Mitchum R., Campion K. & Rahmanian V. 1990: Siliciclastic Sequence Stratigraphy in Well Logs, Cores, and Outcrops. *AAPG Methods in Exploration* 7, 1–55.

Wood G.D., Gabriel A.M. & Lawson J.C. 1996: Palynological techniques — processing and microscopy. In: Jansonius J. & McGregor D.C. (Eds.): Palynology: Principles and Applications. *AASP Foundation* 1, 29–50.

Yanev S. 2000: Palaeozoic terranes of the Balkan Peninsula in the framework of Pangea assembly. *Palaeogeogr. Palaeoclimatol. Palaeoecol.* 161, 151–177.

Zagorchev I. & Budurov K. 2009: Triassic geology. In: Zagorchev I., Dabovski Ch. & Nikolov T. (Eds.): Geology of Bulgaria, vol. 2, Mesozoic geology. *Acad. Publ. "Prof. Marin Drinov"*, Sofia, 39–131.

Zdravkov A., Ajdanlijsky G., Gross D. & Bech A. 2019: Organic petrological and geochemical properties of jet from the middle Triassic Mogila Formation, West Bulgaria. *Geol. Carpath.* 70, 62–74.